

~~SECRET//NOFORN~~

SARS-COV-2 GENOME ANALYSIS

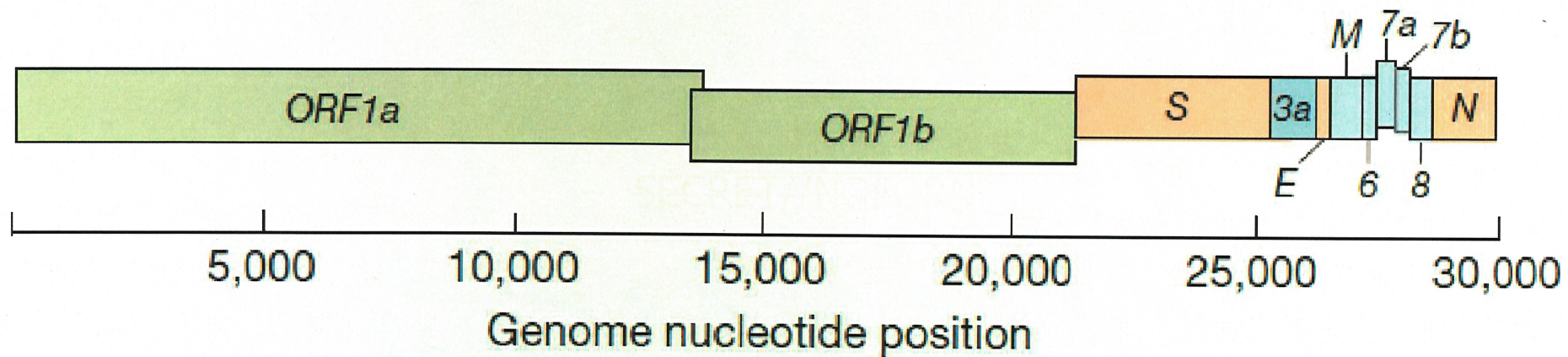
(b)(3):10 USC 424; (b)(6)

June 25, 2020

~~SECRET//NOFORN~~

~~SECRET//NOFORN~~

SARS-CoV-2 Genome



The next two pages are DIF citing (b)(1) and (b)(3)
and are not provided.

~~SECRET//NOFORN~~

~~SECRET//NOFORN~~

Methods to construct a Coronavirus Full-Length Clone

~~SECRET//NOFORN~~

~~SECRET//NOFORN~~

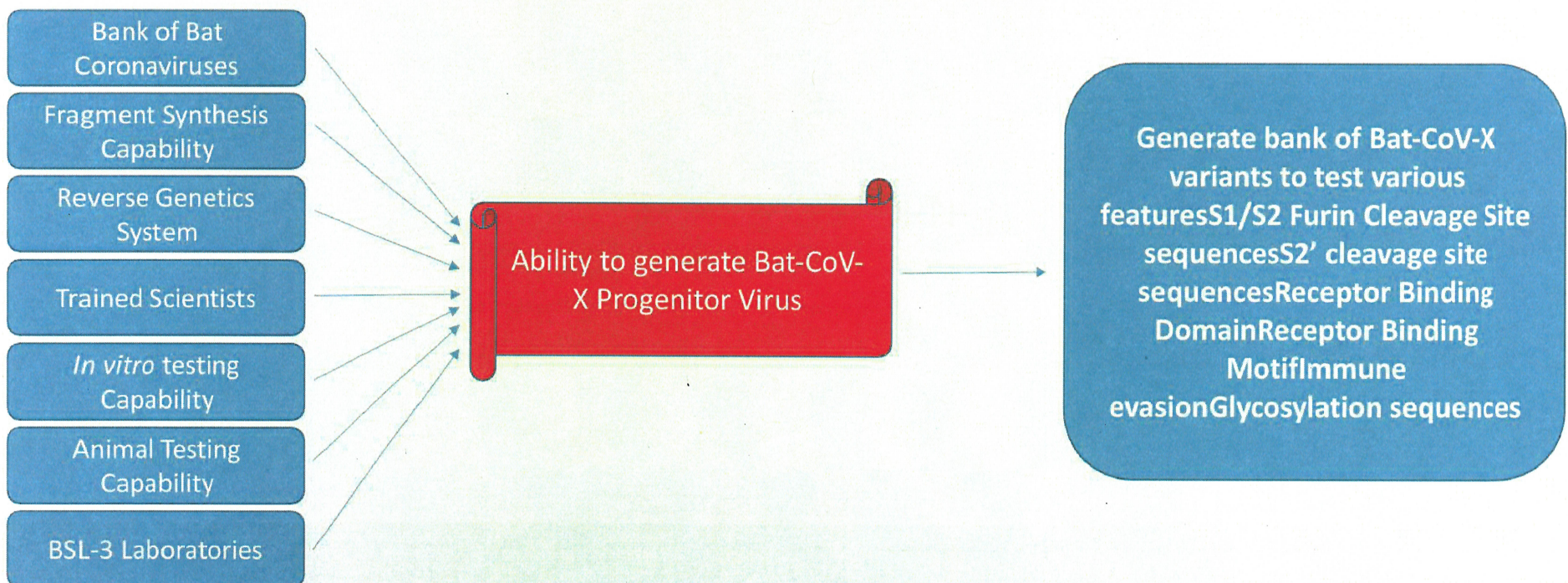
CORONAVIRUS INFECTIOUS CLONE CONSTRUCTION

- 1) Synthesize or PCR amplify 6-10 segments of a Bat CoronavirusBuild a 5' transcription initiation fragment“stitch” the fragments together using an infectious clone technology 3' to the transcription initiation fragmentRestriction-enzyme-based fragment cloning systemOverlapping Fragment systemGuided RNA RecombinationClone in a suitable host (E. coli, yeast, etc.)Sequence verify cloned insert

~~SECRET//NOFORN~~

~~SECRET//NOFORN~~

CAPABILITIES NEEDED TO CONSTRUCT A BAT-LIKE CORONAVIRUS INFECTIOUS CLONE



The next page is DIF citing (b)(1) and (b)(3) and is not provided.

~~SECRET//NOFORN~~

~~SECRET//NOFORN~~

Type IIS Restriction Enzymes and Golden Gate Assembly System

~~SECRET//NOFORN~~

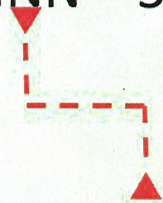
~~SECRET//NOFORN~~

Type IIS Restriction Enzymes

- Non palindromic recognition siteCuts at sites outside of recognition siteEach digested location has unique nucleotide overhangsExampleBsal

5' – GGTCTCNNNN – 3'

3' – CCAGAGNNNN – 5'



~~SECRET//NOFORN~~

~~SECRET//NOFORN~~

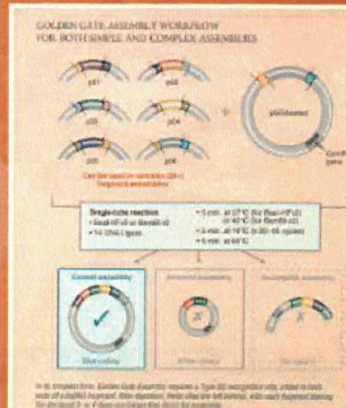
Push the limits of Golden Gate Assembly

Golden Gate Assembly [1,2] allows for the efficient and seamless assembly of DNA fragments using activities of Type IIS restriction enzymes and T4 DNA Ligase.

With constant advances in both the development of new enzymes and research on maximizing enzyme functionality (e.g., ligase fidelity), NEB is the industry leader in pushing the limits of Golden Gate Assembly and related methods.

Advantages:

- Chain seamlessly, with no scars remaining after assembly
- Perform single insert cloning in just 5 minutes using our fast protocols
- Generate libraries with high efficiencies
- Assemble multiple fragments (2-20+) in order, in a single reaction
- Experience high efficiency, even with regions of high GC content and areas of repeats
- Gain with a broad range of fragment sizes (<100 bp to >1.5 kb)



FEATURED PRODUCTS:

Type IIS Restriction Enzymes used in Golden Gate Assembly

Type IIS restriction enzymes recognize asymmetric DNA sequences and cleave outside of their recognition sequence. Type IIS enzymes commonly used in Golden Gate Assembly are listed below. NEB currently offers over 45 Type IIS restriction enzymes.

Please visit www.neb.com for comprehensive table.

PRODUCT	NET #	DESCRIPTION	SIZE
BsaI	RE0001	BSAI(B276)	300U/100 μl
BsaI-HF	RE0002	BSAI(HF)(276)	300U/100 μl
BpuMI	RE0003	BPU(MI)(283)	1,000U/500 μl
BpuMI-HF	RE0004	BPU(MI-HF)(283)	1,000U/500 μl
BpuMI-HF®V2	RE0005	BPU(MI-HF®V2)(283)	1,000U/500 μl
BpuMI-V2	RE0006	BPU(MI-V2)(283)	1,000U/500 μl
BpuMI-V2	RE0007	BPU(MI-V2)(283)	1,000U/500 μl
BpuMI-V2	RE0008	BPU(MI-V2)(283)	1,000U/500 μl
BpuMI-V2	RE0009	BPU(MI-V2)(283)	1,000U/500 μl
BpuMI-V2	RE0010	BPU(MI-V2)(283)	1,000U/500 μl
BpuMI-V2	RE0011	BPU(MI-V2)(283)	1,000U/500 μl
BpuMI-V2	RE0012	BPU(MI-V2)(283)	1,000U/500 μl
BpuMI-V2	RE0013	BPU(MI-V2)(283)	1,000U/500 μl
BpuMI-V2	RE0014	BPU(MI-V2)(283)	1,000U/500 μl
BpuMI-V2	RE0015	BPU(MI-V2)(283)	1,000U/500 μl
BpuMI-V2	RE0016	BPU(MI-V2)(283)	1,000U/500 μl
BpuMI-V2	RE0017	BPU(MI-V2)(283)	1,000U/500 μl
BpuMI-V2	RE0018	BPU(MI-V2)(283)	1,000U/500 μl
BpuMI-V2	RE0019	BPU(MI-V2)(283)	1,000U/500 μl
BpuMI-V2	RE0020	BPU(MI-V2)(283)	1,000U/500 μl
BpuMI-V2	RE0021	BPU(MI-V2)(283)	1,000U/500 μl
BpuMI-V2	RE0022	BPU(MI-V2)(283)	1,000U/500 μl
BpuMI-V2	RE0023	BPU(MI-V2)(283)	1,000U/500 μl
BpuMI-V2	RE0024	BPU(MI-V2)(283)	1,000U/500 μl
BpuMI-V2	RE0025	BPU(MI-V2)(283)	1,000U/500 μl
BpuMI-V2	RE0026	BPU(MI-V2)(283)	1,000U/500 μl
BpuMI-V2	RE0027	BPU(MI-V2)(283)	1,000U/500 μl
BpuMI-V2	RE0028	BPU(MI-V2)(283)	1,000U/500 μl
BpuMI-V2	RE0029	BPU(MI-V2)(283)	1,000U/500 μl
BpuMI-V2	RE0030	BPU(MI-V2)(283)	1,000U/500 μl
BpuMI-V2	RE0031	BPU(MI-V2)(283)	1,000U/500 μl
BpuMI-V2	RE0032	BPU(MI-V2)(283)	1,000U/500 μl
BpuMI-V2	RE0033	BPU(MI-V2)(283)	1,000U/500 μl
BpuMI-V2	RE0034	BPU(MI-V2)(283)	1,000U/500 μl
BpuMI-V2	RE0035	BPU(MI-V2)(283)	1,000U/500 μl
BpuMI-V2	RE0036	BPU(MI-V2)(283)	1,000U/500 μl
BpuMI-V2	RE0037	BPU(MI-V2)(283)	1,000U/500 μl
BpuMI-V2	RE0038	BPU(MI-V2)(283)	1,000U/500 μl
BpuMI-V2	RE0039	BPU(MI-V2)(283)	1,000U/500 μl
BpuMI-V2	RE0040	BPU(MI-V2)(283)	1,000U/500 μl
BpuMI-V2	RE0041	BPU(MI-V2)(283)	1,000U/500 μl
BpuMI-V2	RE0042	BPU(MI-V2)(283)	1,000U/500 μl
BpuMI-V2	RE0043	BPU(MI-V2)(283)	1,000U/500 μl
BpuMI-V2	RE0044	BPU(MI-V2)(283)	1,000U/500 μl
BpuMI-V2	RE0045	BPU(MI-V2)(283)	1,000U/500 μl
BpuMI-V2	RE0046	BPU(MI-V2)(283)	1,000U/500 μl
BpuMI-V2	RE0047	BPU(MI-V2)(283)	1,000U/500 μl
BpuMI-V2	RE0048	BPU(MI-V2)(283)	1,000U/500 μl
BpuMI-V2	RE0049	BPU(MI-V2)(283)	1,000U/500 μl
BpuMI-V2	RE0050	BPU(MI-V2)(283)	1,000U/500 μl
BpuMI-V2	RE0051	BPU(MI-V2)(283)	1,000U/500 μl
BpuMI-V2	RE0052	BPU(MI-V2)(283)	1,000U/500 μl
BpuMI-V2	RE0053	BPU(MI-V2)(283)	1,000U/500 μl
BpuMI-V2	RE0054	BPU(MI-V2)(283)	1,000U/500 μl
BpuMI-V2	RE0055	BPU(MI-V2)(283)	1,000U/500 μl
BpuMI-V2	RE0056	BPU(MI-V2)(283)	1,000U/500 μl
BpuMI-V2	RE0057	BPU(MI-V2)(283)	1,000U/500 μl
BpuMI-V2	RE0058	BPU(MI-V2)(283)	1,000U/500 μl
BpuMI-V2	RE0059	BPU(MI-V2)(283)	1,000U/500 μl
BpuMI-V2	RE0060	BPU(MI-V2)(283)	1,000U/500 μl
BpuMI-V2	RE0061	BPU(MI-V2)(283)	1,000U/500 μl
BpuMI-V2	RE0062	BPU(MI-V2)(283)	1,000U/500 μl
BpuMI-V2	RE0063	BPU(MI-V2)(283)	1,000U/500 μl
BpuMI-V2	RE0064	BPU(MI-V2)(283)	1,000U/500 μl
BpuMI-V2	RE0065	BPU(MI-V2)(283)	1,000U/500 μl
BpuMI-V2	RE0066	BPU(MI-V2)(283)	1,000U/500 μl
BpuMI-V2	RE0067	BPU(MI-V2)(283)	1,000U/500 μl
BpuMI-V2	RE0068	BPU(MI-V2)(283)	1,000U/500 μl
BpuMI-V2	RE0069	BPU(MI-V2)(283)	1,000U/500 μl
BpuMI-V2	RE0070	BPU(MI-V2)(283)	1,000U/500 μl
BpuMI-V2	RE0071	BPU(MI-V2)(283)	1,000U/500 μl
BpuMI-V2	RE0072	BPU(MI-V2)(283)	1,000U/500 μl
BpuMI-V2	RE0073	BPU(MI-V2)(283)	1,000U/500 μl
BpuMI-V2	RE0074	BPU(MI-V2)(283)	1,000U/500 μl
BpuMI-V2	RE0075	BPU(MI-V2)(283)	1,000U/500 μl
BpuMI-V2	RE0076	BPU(MI-V2)(283)	1,000U/500 μl
BpuMI-V2	RE0077	BPU(MI-V2)(283)	1,000U/500 μl
BpuMI-V2	RE0078	BPU(MI-V2)(283)	1,000U/500 μl
BpuMI-V2	RE0079	BPU(MI-V2)(283)	1,000U/500 μl
BpuMI-V2	RE0080	BPU(MI-V2)(283)	1,000U/500 μl
BpuMI-V2	RE0081	BPU(MI-V2)(283)	1,000U/500 μl
BpuMI-V2	RE0082	BPU(MI-V2)(283)	1,000U/500 μl
BpuMI-V2	RE0083	BPU(MI-V2)(283)	1,000U/500 μl
BpuMI-V2	RE0084	BPU(MI-V2)(283)	1,000U/500 μl
BpuMI-V2	RE0085	BPU(MI-V2)(283)	1,000U/500 μl
BpuMI-V2	RE0086	BPU(MI-V2)(283)	1,000U/500 μl
BpuMI-V2	RE0087	BPU(MI-V2)(283)	1,000U/500 μl
BpuMI-V2	RE0088	BPU(MI-V2)(283)	1,000U/500 μl
BpuMI-V2	RE0089	BPU(MI-V2)(283)	1,000U/500 μl
BpuMI-V2	RE0090	BPU(MI-V2)(283)	1,000U/500 μl
BpuMI-V2	RE0091	BPU(MI-V2)(283)	1,000U/500 μl
BpuMI-V2	RE0092	BPU(MI-V2)(283)	1,000U/500 μl
BpuMI-V2	RE0093	BPU(MI-V2)(283)	1,000U/500 μl
BpuMI-V2	RE0094	BPU(MI-V2)(283)	1,000U/500 μl
BpuMI-V2	RE0095	BPU(MI-V2)(283)	1,000U/500 μl
BpuMI-V2	RE0096	BPU(MI-V2)(283)	1,000U/500 μl
BpuMI-V2	RE0097	BPU(MI-V2)(283)	1,000U/500 μl
BpuMI-V2	RE0098	BPU(MI-V2)(283)	1,000U/500 μl
BpuMI-V2	RE0099	BPU(MI-V2)(283)	1,000U/500 μl
BpuMI-V2	RE0100	BPU(MI-V2)(283)	1,000U/500 μl
BpuMI-V2	RE0101	BPU(MI-V2)(283)	1,000U/500 μl
BpuMI-V2	RE0102	BPU(MI-V2)(283)	1,000U/500 μl
BpuMI-V2	RE0103	BPU(MI-V2)(283)	1,000U/500 μl
BpuMI-V2	RE0104	BPU(MI-V2)(283)	1,000U/500 μl
BpuMI-V2	RE0105	BPU(MI-V2)(283)	1,000U/500 μl
BpuMI-V2	RE0106	BPU(MI-V2)(283)	1,000U/500 μl
BpuMI-V2	RE0107	BPU(MI-V2)(283)	1,000U/500 μl
BpuMI-V2	RE0108	BPU(MI-V2)(283)	1,000U/500 μl
BpuMI-V2	RE0109	BPU(MI-V2)(283)	1,000U/500 μl
BpuMI-V2	RE0110	BPU(MI-V2)(283)	1,000U/500 μl
BpuMI-V2	RE0111	BPU(MI-V2)(283)	1,000U/500 μl
BpuMI-V2	RE0112	BPU(MI-V2)(283)	1,000U/500 μl
BpuMI-V2	RE0113	BPU(MI-V2)(283)	1,000U/500 μl
BpuMI-V2	RE0114	BPU(MI-V2)(283)	1,000U/500 μl
BpuMI-V2	RE0115	BPU(MI-V2)(283)	1,000U/500 μl
BpuMI-V2	RE0116	BPU(MI-V2)(283)	1,000U/500 μl
BpuMI-V2	RE0117	BPU(MI-V2)(283)	1,000U/500 μl
BpuMI-V2	RE0118	BPU(MI-V2)(283)	1,000U/500 μl
BpuMI-V2	RE0119	BPU(MI-V2)(283)	1,000U/500 μl
BpuMI-V2	RE0120	BPU(MI-V2)(283)	1,000U/500 μl
BpuMI-V2	RE0121	BPU(MI-V2)(283)	1,000U/500 μl
BpuMI-V2	RE0122	BPU(MI-V2)(283)	1,000U/500 μl
BpuMI-V2	RE0123	BPU(MI-V2)(283)	1,000U/500 μl
BpuMI-V2	RE0124	BPU(MI-V2)(283)	1,000U/500 μl
BpuMI-V2	RE0125	BPU(MI-V2)(283)	1,000U/500 μl
BpuMI-V2	RE0126	BPU(MI-V2)(283)	1,000U/500 μl
BpuMI-V2	RE0127	BPU(MI-V2)(283)	1,000U/500 μl
BpuMI-V2	RE0128	BPU(MI-V2)(283)	1,000U/500 μl
BpuMI-V2	RE0129	BPU(MI-V2)(283)	1,000U/500 μl
BpuMI-V2	RE0130	BPU(MI-V2)(283)	1,000U/500 μl
BpuMI-V2	RE0131	BPU(MI-V2)(283)	1,000U/500 μl
BpuMI-V2	RE0132	BPU(MI-V2)(283)	1,000U/500 μl
BpuMI-V2	RE0133	BPU(MI-V2)(283)	1,000U/500 μl
BpuMI-V2	RE0134	BPU(MI-V2)(283)	1,000U/500 μl
BpuMI-V2	RE0135	BPU(MI-V2)(283)	1,000U/500 μl
BpuMI-V2	RE0136	BPU(MI-V2)(283)	1,000U/500 μl
BpuMI-V2	RE0137	BPU(MI-V2)(283)	1,000U/500 μl
BpuMI-V2	RE0138	BPU(MI-V2)(283)	1,000U/500 μl
BpuMI-V2	RE0139	BPU(MI-V2)(283)	1,000U/500 μl
BpuMI-V2	RE0140	BPU(MI-V2)(283)	1,000U/500 μl
BpuMI-V2	RE0141	BPU(MI-V2)(283)	1,000U/500 μl
BpuMI-V2	RE0142	BPU(MI-V2)(283)	1,000U/500 μl
BpuMI-V2	RE0143	BPU(MI-V2)(283)	1,000U/500 μl
BpuMI-V2	RE0144	BPU(MI-V2)(283)	1,000U/500 μl
BpuMI-V2	RE0145	BPU(MI-V2)(283)	1,000U/500 μl
BpuMI-V2	RE0146	BPU(MI-V2)(283)	1,000U/500 μl
BpuMI-V2	RE0147	BPU(MI-V2)(283)	1,000U/500 μl
BpuMI-V2	RE0148	BPU(MI-V2)(283)	1,000U/500 μl
BpuMI-V2	RE0149	BPU(MI-V2)(283)	1,000U/500 μl
BpuMI-V2	RE0150	BPU(MI-V2)(283)	1,000U/500 μl
BpuMI-V2	RE0151	BPU(MI-V2)(283)	1,000U/500 μl
BpuMI-V2	RE0152	BPU(MI-V2)(283)	1,000U/500 μl
BpuMI-V2	RE0153	BPU(MI-V2)(283)	1,000U/500 μl
BpuMI-V2	RE0154	BPU(MI-V2)(283)	1,000U/500 μl
BpuMI-V2	RE0155	BPU(MI-V2)(283)	1,000U/500 μl
BpuMI-V2	RE0156	BPU(MI-V2)(283)	1,000U/500 μl
BpuMI-V2	RE0157	BPU(MI-V2)(283)	1,000U/500 μl
BpuMI-V2	RE0158	BPU(MI-V2)(283)	1,000U/500 μl
BpuMI-V2	RE0159	BPU(MI-V2)(283)	1,000U/500 μl
BpuMI-V2	RE0160	BPU(MI-V2)(283)	1,000U/500 μl
BpuMI-V2	RE0161	BPU(MI-V2)(283)	1,000U/500 μl
BpuMI-V2	RE0162	BPU(MI-V2)(283)	1,000U/500 μl
BpuMI-V2	RE0163	BPU(MI-V2)(283)	1,000U/500 μl
BpuMI-V2	RE0164	BPU(MI-V2)(283)	1,000U/500 μl
BpuMI-V2	RE0165	BPU(MI-V2)(283)	1,000U/500 μl
BpuMI-V2	RE0166	BPU(MI-V2)(283)	1,000U/500 μl
BpuMI-V2	RE0167	BPU(MI-V2)(283)	1,000U/500 μl
BpuMI-V2	RE0168	BPU(MI-V2)(283)	1,000U/500 μl
BpuMI-V2	RE0169	BPU(MI-V2)(283)	1,000U/500 μl
BpuMI-V2	RE0170	BPU(MI-V2)(283)	1,000U/500 μl
BpuMI-V2	RE0171	BPU(MI-V2)(283)	1,000U/500 μl
BpuMI-V2	RE0172	BPU(MI-V2)(283)	1,000U/500 μl
BpuMI-V2	RE0173	BPU(MI-V2)(283)	1,000U/500 μl
BpuMI-V2	RE0174	BPU(MI-V2)(283)	1,000U/500 μl
BpuMI-V2	RE0175	BPU(MI-V2)(283)	1,000U/500 μl
BpuMI-V2	RE0176	BPU(MI-V2)(283)	1,000U/500 μl
BpuMI-V2	RE0177	BPU(MI-V2)(283)	1,000U/500 μl
BpuMI-V2	RE0178	BPU(MI-V2)(283)	1,000U/500 μl
BpuMI-V2	RE0179	BPU(MI-V2)(283)	1,000U/500 μl
BpuMI-V2	RE0180	BPU(MI-V2)(283)	1,000U/500 μl
BpuMI-V2	RE0181	BPU(MI-V2)(283)	1,000U/500 μl
BpuMI-V2	RE0182	BPU(MI-V2)(283)	1,000U/500 μl
BpuMI-V2	RE0183	BPU(MI-V2)(283)	1,000U/500 μl
BpuMI-V2	RE0184	BPU(MI-V2)(283)	1,000U/500 μl
BpuMI-V2	RE0185	BPU(MI-V2)(283)	1,000U/500 μl
BpuMI-V2	RE0186	BPU(MI-V2)(283)</td	

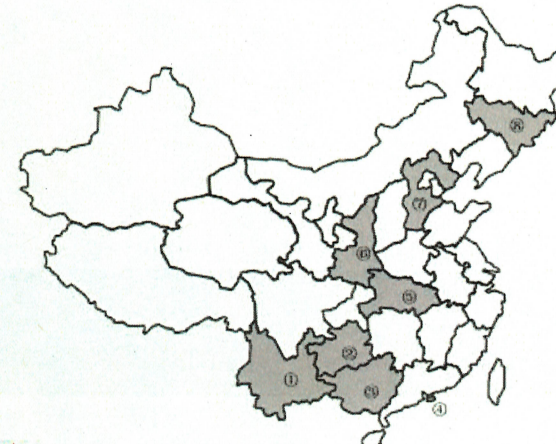
~~SECRET//NOFORN~~

WIV Bat Coronavirus Collection Efforts

- WIV possesses a large bank of Bat Coronaviruses isolated from various bat species in Yunnan Province China Ge et al., 2013 Yang et al., 2016 Hu et al., 2017 Five-year longitudinal study to isolate Bat Coronaviruses (April 2011 – October 2015) Only a few sequences have been published

Table 1. Summary of SARSr-CoV detection in bats from a single habitat in Kunming, Yunnan.

Sampling time	Sample type	Sample Numbers			SARSr-CoV + bat species (No.)
		Total	CoV +	SARSr-CoV +	
April, 2011	anal swab	14	1	1	<i>R. sinicus</i> (1)
October, 2011	anal swab	8	3	3	<i>R. sinicus</i> (3)
May, 2012	anal swab & feces	54	9	4	<i>R. sinicus</i> (4)
September, 2012	feces	39	20	19	<i>R. sinicus</i> (16) <i>R. ferrumequinum</i> (3)
April, 2013	feces	52	21	16	<i>R. sinicus</i> (16)
July, 2013	anal swab & feces	115	9	8	<i>R. sinicus</i> (8)
May, 2014	feces	131	8	4	<i>A. stoliczkanus</i> (3) <i>R. affinis</i> (1)
October, 2014	anal swab	19	4	4	<i>R. sinicus</i> (4)
May, 2015	feces	145	3	0	
October, 2015	anal swab	25	6	5	<i>R. sinicus</i> (5) <i>R. (61) A</i> (3)
Total		602	84	64	



- ① Yunnan
- ② Guizhou
- ③ Guangxi
- ④ Hong Kong
- ⑤ Hubei
- ⑥ Shaanxi
- ⑦ Hebei
- ⑧ Jilin

The next page is DIF citing (b)(1) and (b)(3) and is not provided.

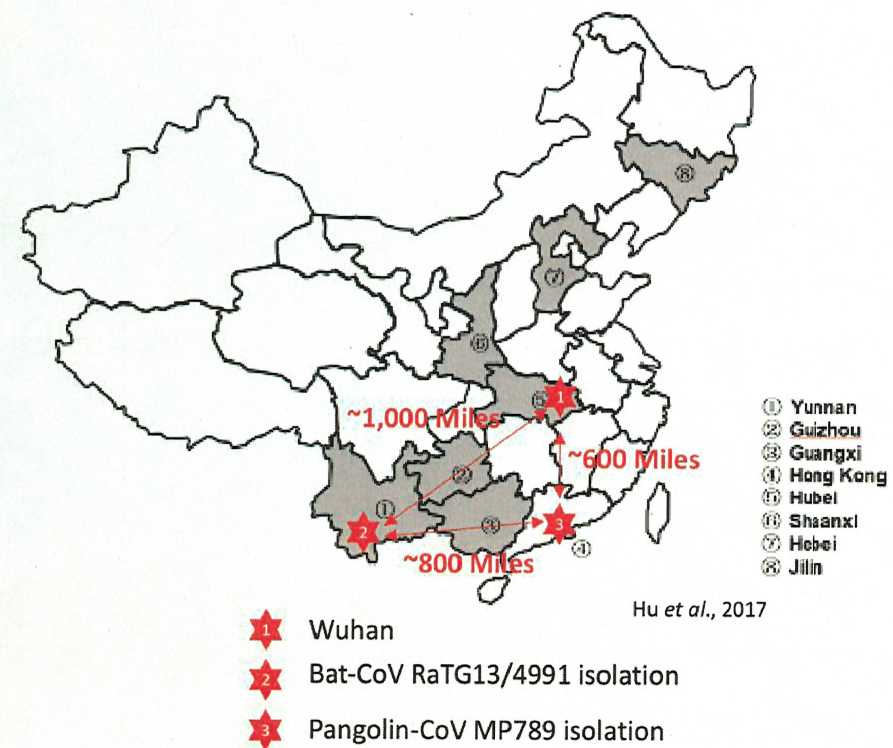
~~SECRET//NOFORN~~

Extracted from Hu et al., 2017

~~SECRET//NOFORN~~

Isolation Locations for RaTG13 and MP789

- RaTG13/4991 isolated from a cave in Yunnan ProvinceRaTG13/4991 is a RdRp lineage 1 BetaCoVMP789 was isolated from diseased Pangolins in Guangdong ProvinceMP789 is a RdRp lineage 2 BetaCoV~800 miles separate these two locationsWIV also collected CoV's from Guandong and may have a MP789-related virus in their bank“All the genomic constituents of SARS-CoV including the hypervariable regions S and ORF8 were discovered from different bat SARSr-CoVs in the same cave in Yunnan, with evidence of recombination events detected between these bat SARSr-CoVs...” (Yu et al., 2019)Question: How would a Pangolin RBD from 800 miles away in Guangdong Province recombine into a BatCoV in Yunnan Province?



~~SECRET//NOFORN~~

~~SECRET//NOFORN~~

Postulated WIV Bat-CoV-X Full-length Clone Construction Process

~~SECRET//NOFORN~~

~~SECRET//NOFORN~~

Quote from Zeng *et al.*, 2016

- From Materials and Methods, Virus and cells section

"All experiments using live virus was conducted under biosafety level 2 (BSL2) conditions."

From the first paragraph of the Discussion

"In this study, we have developed a fast and cost-effective method for reverse genetics of coronaviruses by combining two approaches developed by others (29, 30). Our method allows the genomes of coronaviruses to be split into multiple fragments and inserted into a BAC plasmid with a single step. Recombinant viruses can then be efficiently rescued by direct transfection of the BAC construct. As the genomes can be divided into multiple short fragments, mutations can be introduced into individual fragments easily (31). Using this method, we successfully rescued three recombinant viruses derived from SL-CoV WIV1 (rWIV1, rWIV1-DX, and rWIV1-GFP-DX)."

The next page is DIF citing (b)(1) and (b)(3) and is not provided.

~~SECRET//NOFORN~~

~~SECRET//NOFORN~~

WIV SARS-CoV Reverse Genetics System

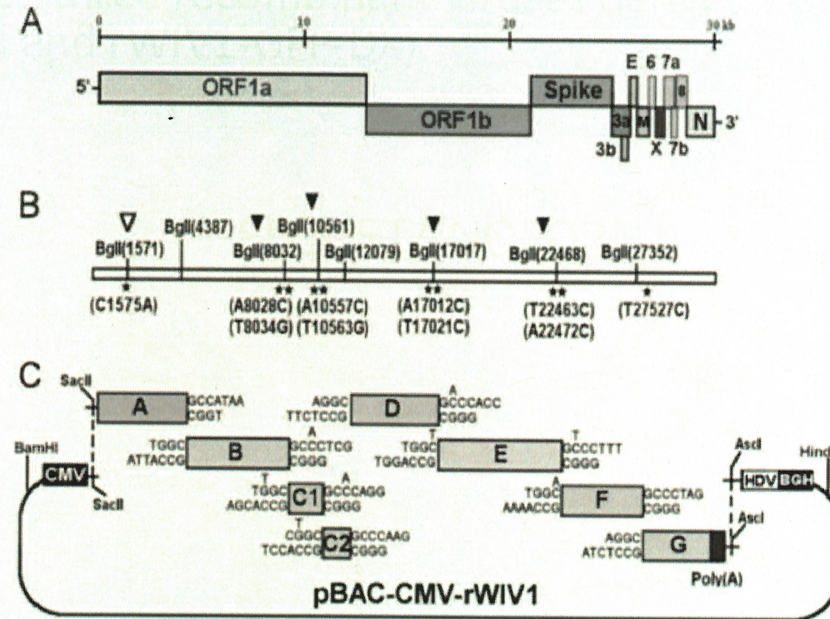
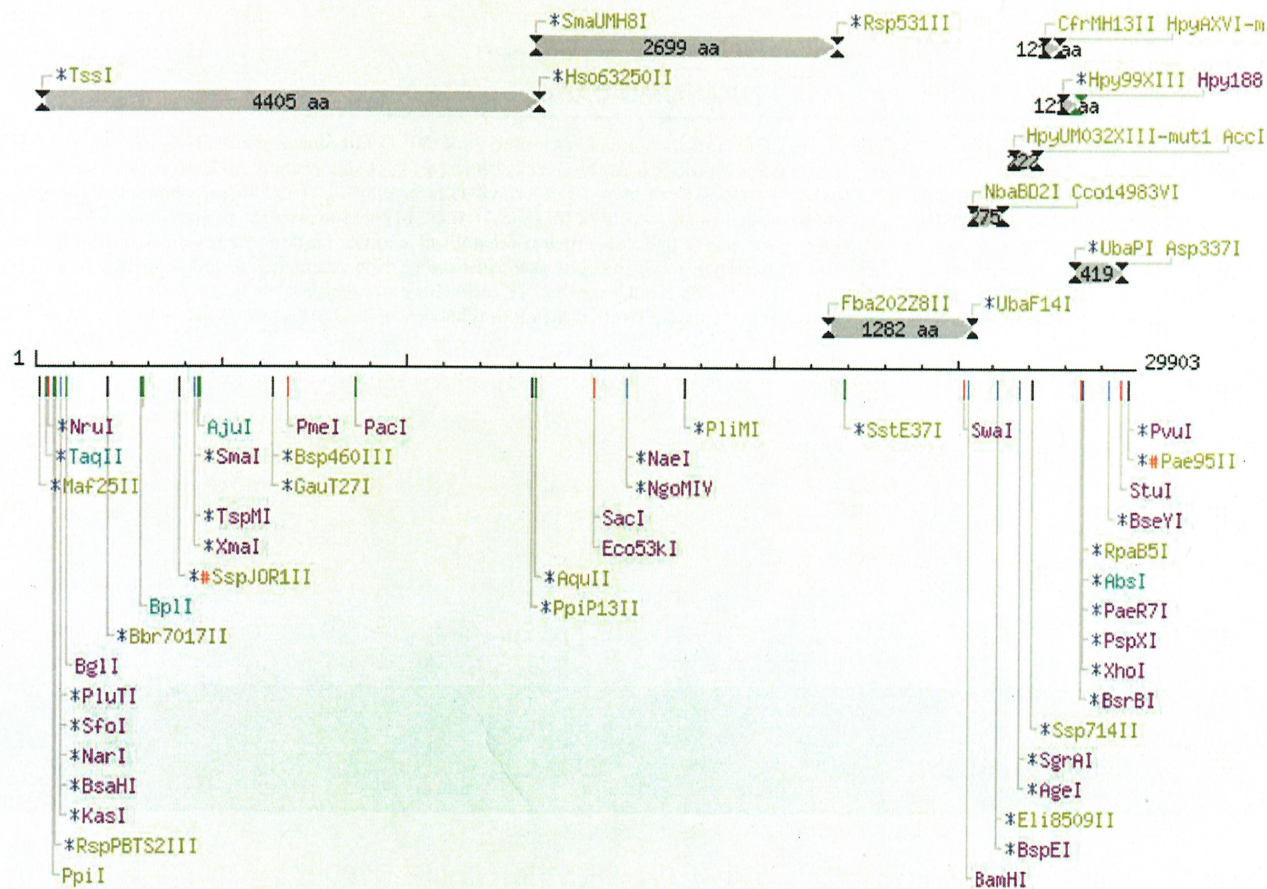


FIG 1 Strategy for construction of an infectious WIV1 BAC clone. (A) Genomic structure of WIV1. (B) The mutations are indicated under the stars. C1575A was used to ablate a natural BgII site at nucleotide 1571 (∇), and T27527C was used to disrupt a potential T7 stop site. The others were for introducing BgII sites (\blacktriangledown). (C) The WIV1 genome was split into eight contiguous cDNAs (A to G): A, nt 1 to 4387; B, nt 4388 to 8032; C1, nt 8033 to 10561; C2, nt 10562 to 12079; D, nt 12080 to 17017; E, nt 17018 to 22468; F, nt 22469 to 27352; G, nt 27353 to 30309. Unique BgII sites were introduced into the fragments by synonymous mutations to make these fragments capable of unidirectional ligation along with native BgII sites in the genome. The original nucleotides are shown above the flanking sequences of corresponding fragments. A poly(A) sequence was added to the 3' terminus of fragment G. A CMV promoter, HDV ribozyme, and BGH transcriptional terminal signal were inserted into pBeloBAC11 between BamHI and HindIII sites. SacII and Ascl sites were introduced between the CMV promoter and ribozyme. Fragments A to G were inserted into the pBAC-CMV plasmid in a single step.

~~SECRET//NOFORN~~

SARS-COV-2 GENOME RESTRICTION MAP



~~SECRET//NOFORN~~

Type IIS Restriction Enzymes

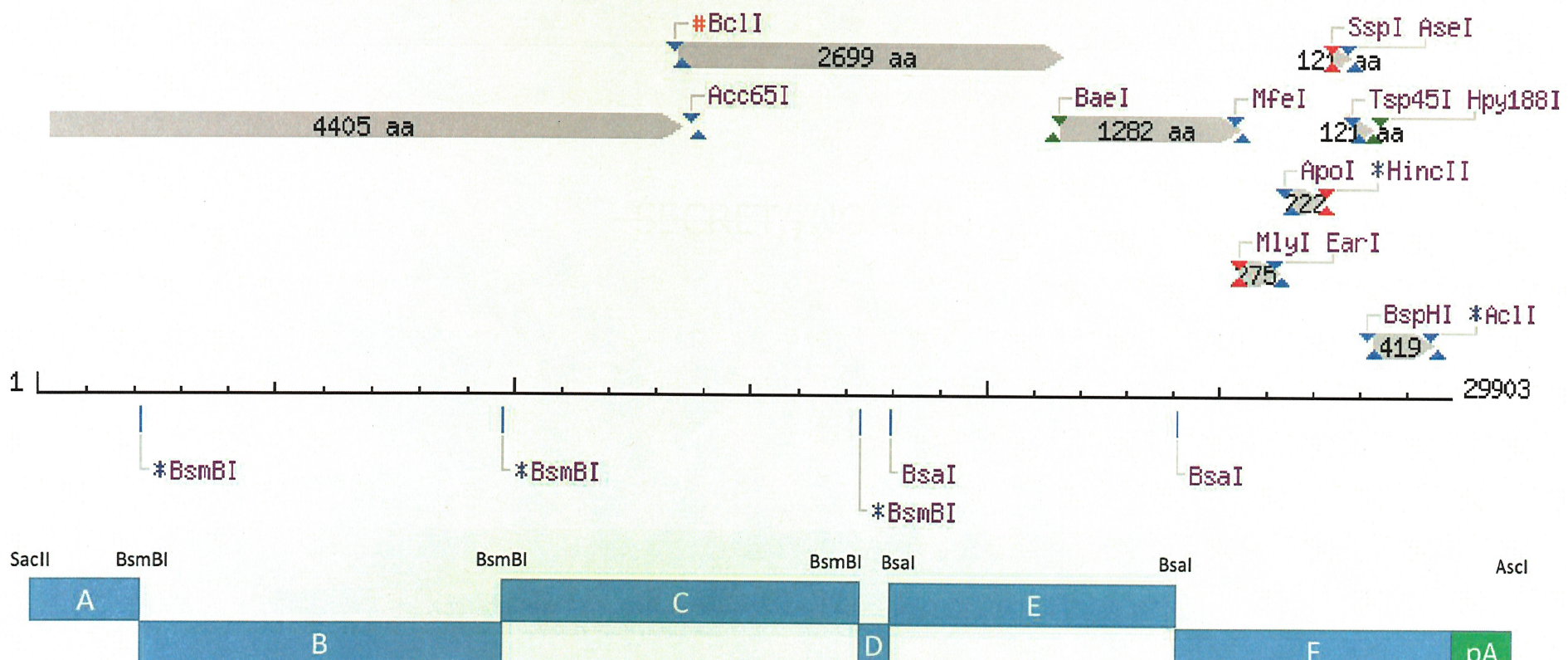
- BsmBI (Plus strand)
5' - CGTCTC_{NNNN}-3'
3' - GCAGAG_{NNNN} - 5' BsaP' (Plus strand)
- BsmBI (Minus strand)
5' - NNNNGAGACG-3'
3' - GGTCTC_{NNNN}-3'
5' BsAI (Minus strand)
3' - CCAGAG_{NNNN} - 5' SARS-CoV-2 genome does not have any SacII or AscI restriction sites

(b)(1); (b)(3)50 USC 3024(i); Sec. 1.4(c); Sec. 1.4(e)

~~SECRET//NOFORN~~

~~SECRET//NOFORN~~

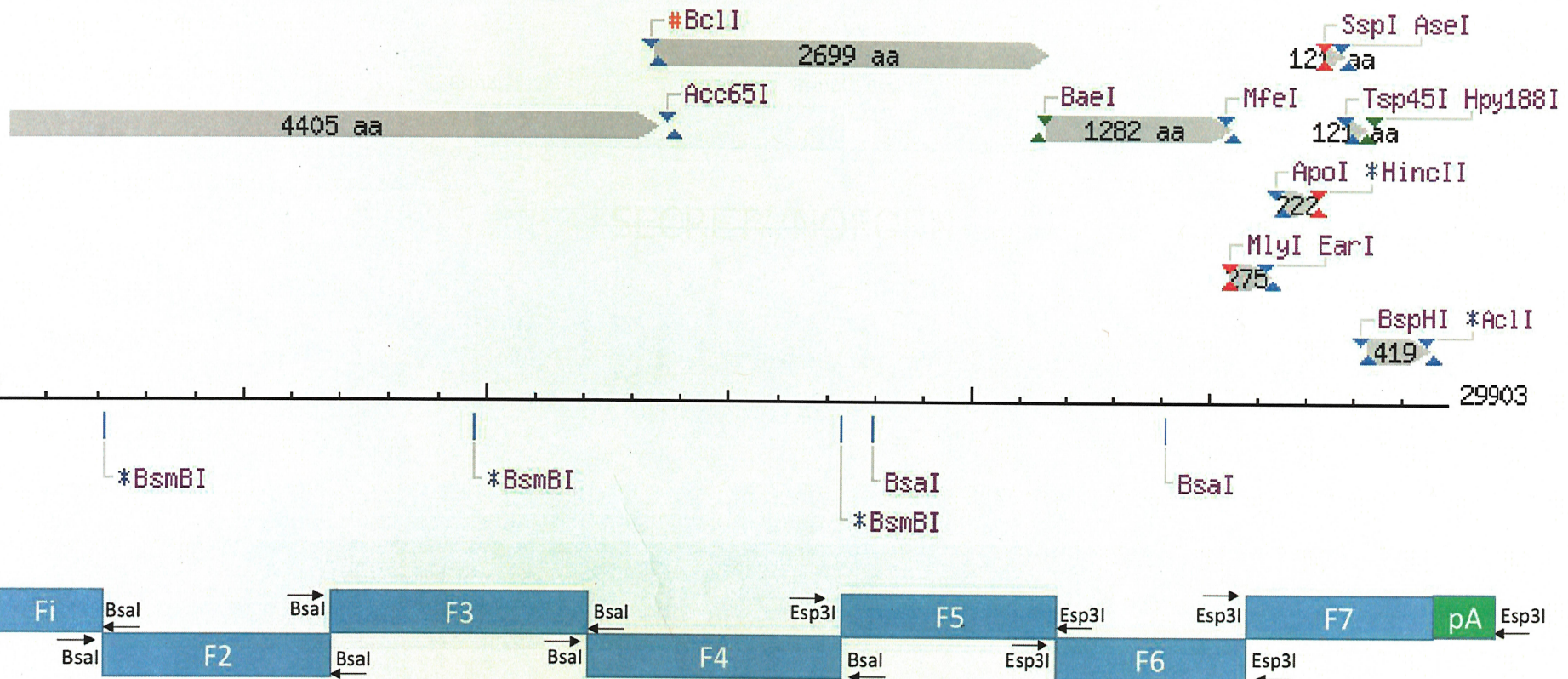
RE-based Fragment Build Option – *BsmBI/Bsal* (4 nt overhangs)



~~SECRET//NOFORN~~

~~SECRET//NOFORN~~

RE-based Fragment Build Option – *Bsal/Esp3I* (Invisible restriction sites)



Xie et al., 2020

~~SECRET//NOFORN~~

~~SECRET//NOFORN~~

Xie et al., 2020 SARS-CoV-2 FLC Assembly

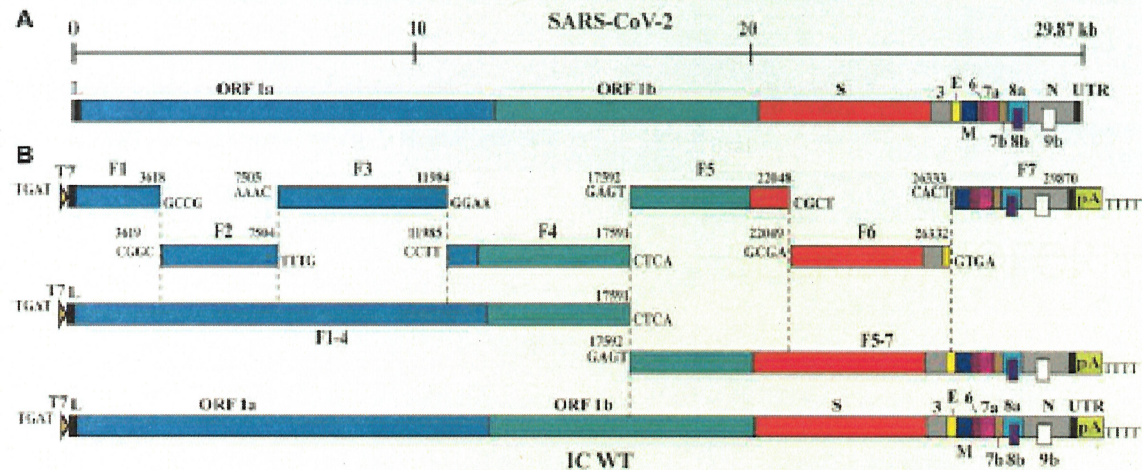


Figure 1. Assembly of a Full-Length SARS-CoV-2 Infection cDNA Clone

(A) Genome structure SARS-CoV-2. The open reading frames (ORFs) from the full genome are indicated.

(B) Strategy for *in vitro* assembly of an infectious cDNA clone of SARS-CoV-2. The nucleotide sequences and genome locations of the cohesive overhangs are indicated. The WT full-length (FL) cDNA of SARS-CoV-2 (IC WT) was directionally assembled using *in vitro* ligation.

(C) Diagram of the terminal sequences of each cDNA fragment recognized by *BsaI* and *EspI*.

(D) Gel analysis of the seven purified cDNA fragments. Individual fragments (F1-F7) were digested from corresponding plasmid clones and gel purified. Seven purified cDNA fragments (50–100 ng) were analyzed on a 0.6% native agarose gel. The 1-kb DNA ladders are indicated.

(E) Gel analysis of cDNA ligation products. About 400 ng of purified ligaton product was analyzed on a 0.6% native agarose gel. Triangle indicates the FL cDNA product. Circles indicate the intermediate cDNA products.

(F) Gel analysis of RNA transcripts. About 1 µg of *in-vitro*-transcribed (IVT) RNAs were analyzed on a 0.6% native agarose gel. DNA ladders are indicated. Because this is a native agarose gel, the DNA size is not directly correlated to the RNA size. Triangle indicates the genome-length RNA transcript. Circles show the shorter RNA transcripts.

C Fragment Terminal Sequence

<i>BsaI</i>	17	F1	3039	GGCTCA TGAT CCAGAGT ACTA	CGGC TGAGACC GCGG ACTCTGG
<i>BsaI</i>	3619	F2	7944	GGCTCA GGGC CCAGAGT GGCG	AAACT TGAGACC TTTG ACTCTGG
<i>BsaI</i>	7988	F3	10384	GGCTCA AAAC CCAGAGT TTTC	CTTT TGAGACC GGAA ACTCTGG
<i>BsaI</i>	10983	F4	17581	GGCTCA CTTT CCAGAGT GGAA	GAGTT TGAGACC CTCA ACTCTGG
<i>EspI</i>	17932	F5	22848	GGCTCA GAGT CCAGAGT CTCA	GGGAT TGAGACC GGCT ACTCTGC
<i>EspI</i>	22049	F6	26332	GGCTCA GGGA CCAGAGT CGCT	CACT TGAGACC GTGA ACTCTGC
<i>EspI</i>	26333	F7	28879	GGCTCA CACT CCAGAGT GTCA	AAAA TGAGACC TTTT ACTCTGC

(b)(3):50 USC 3024(i); Sec. 1.4(c); Sec. 1.4(e)

~~SECRET//NOFORN~~

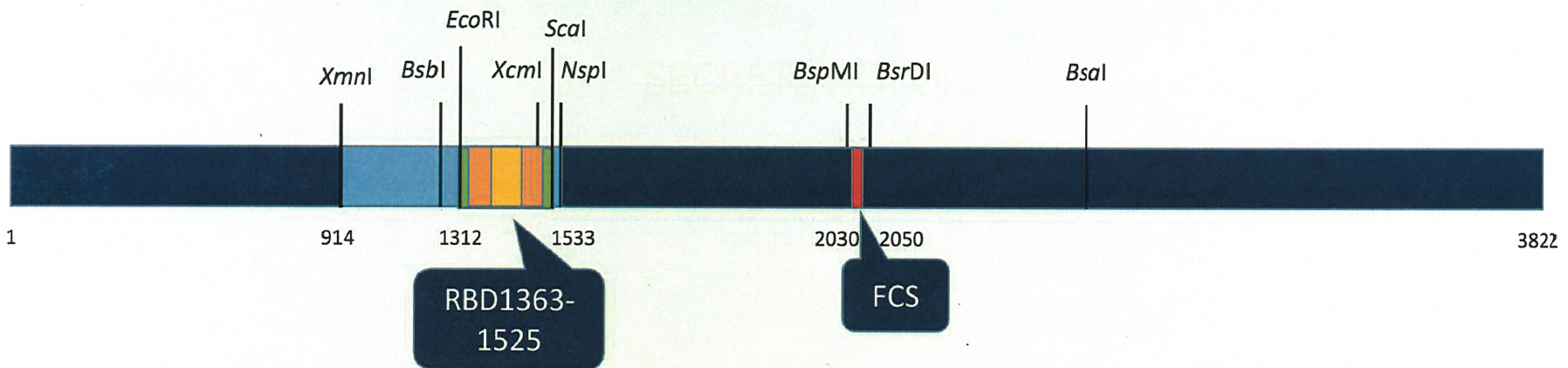
~~SECRET//NOFORN~~

Spike Gene

~~SECRET//NOFORN~~

~~SECRET//NOFORN~~

SARS CoV-2 SPIKE GENE



Highest homology to RaTG13 Pangolin CoV

~~SECRET//NOFORN~~

~~SECRET//NOFORN~~

Spike Gene Swapping Using the WIV SARS-CoV Reverse Genetics System

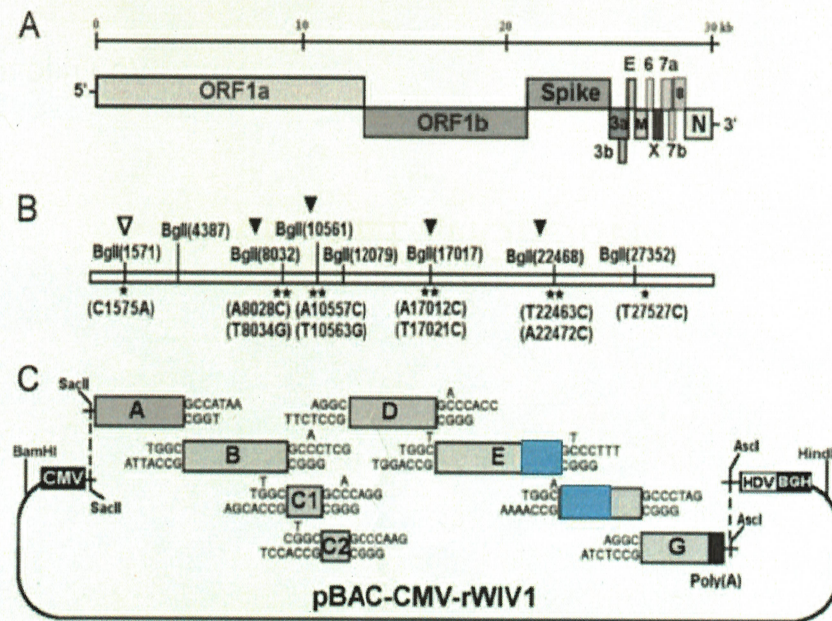


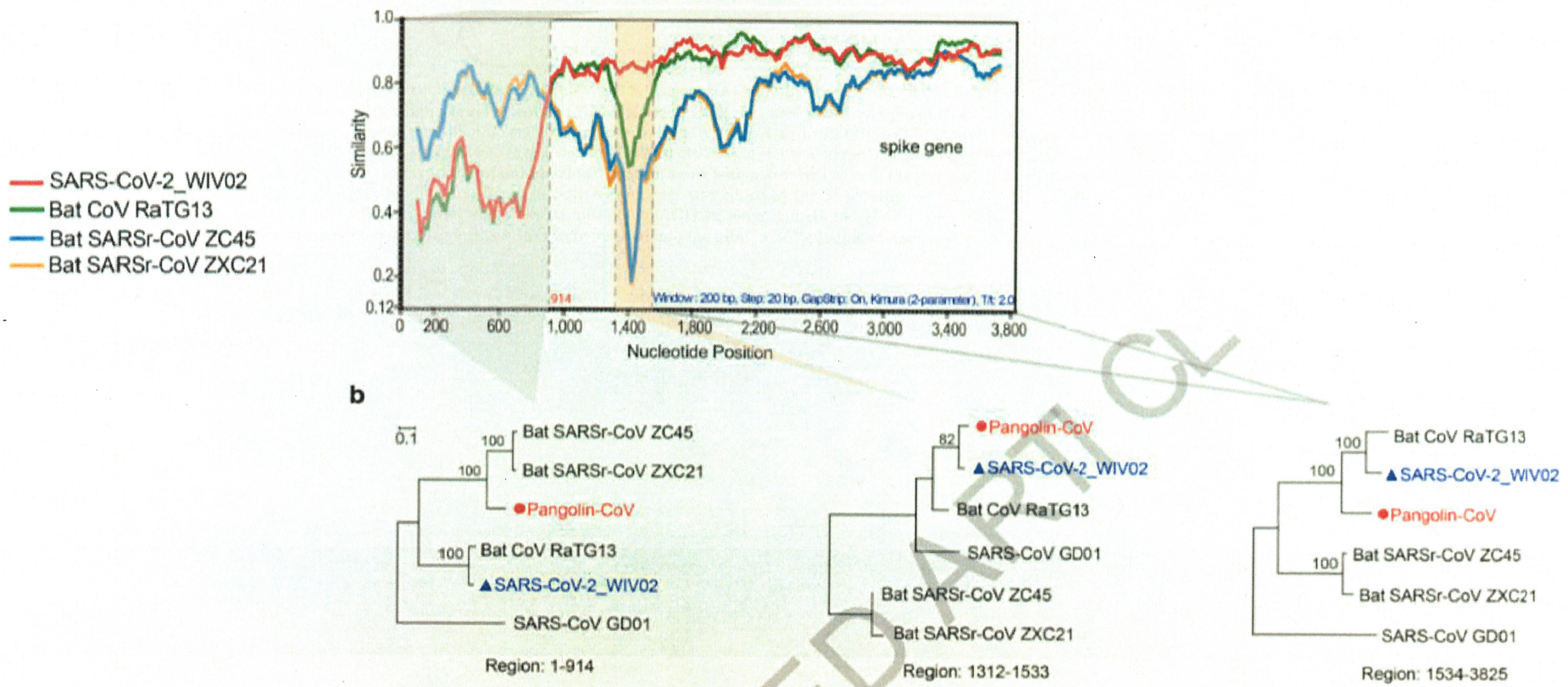
FIG 1 Strategy for construction of an infectious WIV1 BAC clone. (A) Genomic structure of WIV1. (B) The mutations are indicated under the stars. C1575A was used to ablate a natural BgII site at nucleotide 1571 (∇), and T27527C was used to disrupt a potential T7 stop site. The others were for introducing BgII sites (\blacktriangledown). (C) The WIV1 genome was split into eight contiguous cDNAs (A to G): A, nt 1 to 4387; B, nt 4388 to 8032; C1, nt 8033 to 10561; C2, nt 10562 to 12079; D, nt 12080 to 17017; E, nt 17018 to 22468; F, nt 22469 to 27352; G, nt 27353 to 30309. Unique BgII sites were introduced into the fragments by synonymous mutations to make these fragments capable of unidirectional ligation along with native BgII sites in the genome. The original nucleotides are shown above the flanking sequences of corresponding fragments. A poly(A) sequence was added to the 3' terminus of fragment G. A CMV promoter, HDV ribozyme, and BGH transcriptional terminal signal were inserted into pBeloBAC11 between BamHI and HindIII sites. SacII and Ascl sites were introduced between the CMV promoter and ribozyme. Fragments A to G were inserted into the pBAC-CMV plasmid in a single step.

Zeng et al., 2016 Hu et al., 2017

- Hu et al., 2017 swapped out the WIV1 spike gene for the spike gene of the following: Rs4231Rs73 27Rf4075Rs4081Rs40 85Rs4235As6526Rp3

~~SECRET//NOFORN~~

SARS-COV-2 SPIKE GENE SEGMENTS QUERY: PANGOLIN-COV

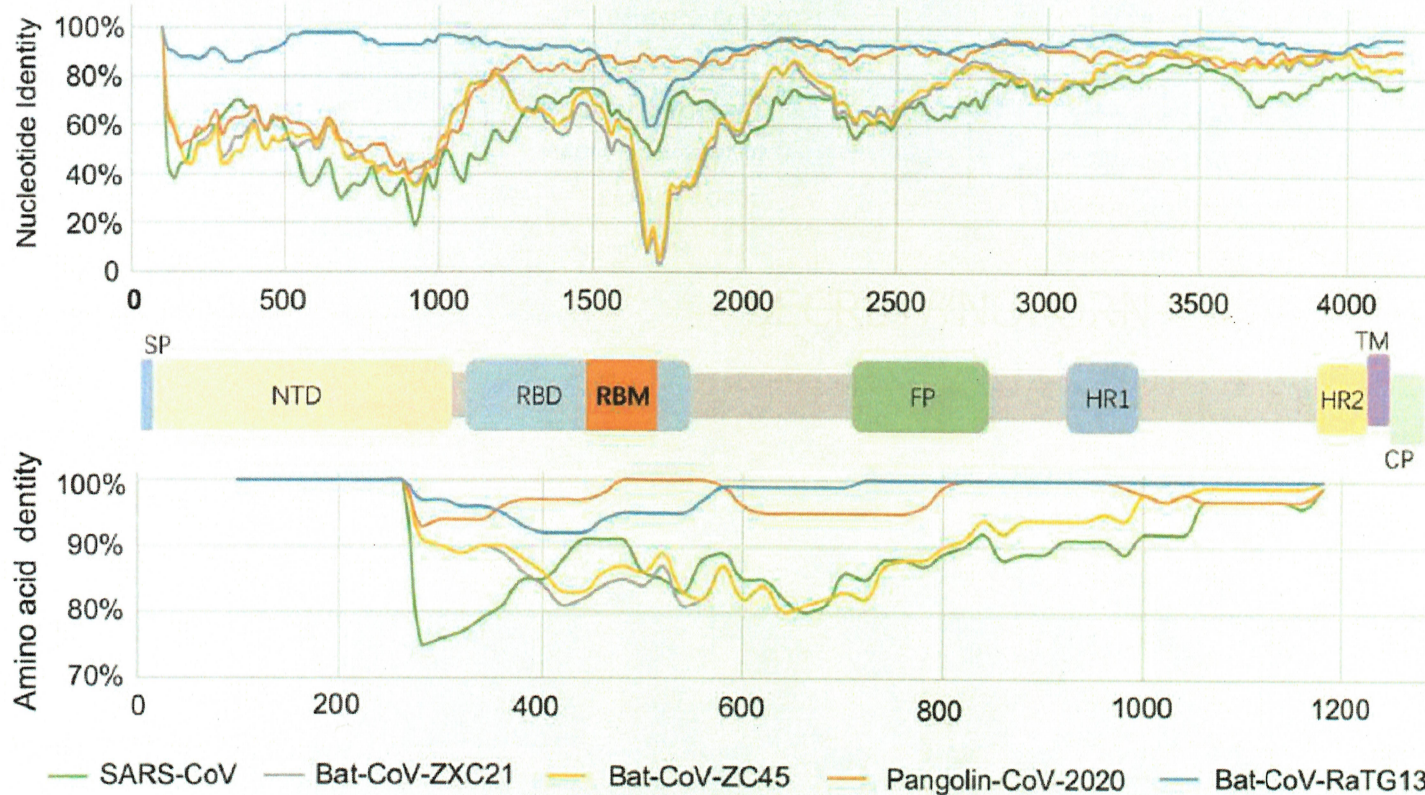


Xiao et al., 2020

~~SECRET//NOFORN~~

~~SECRET//NOFORN~~

SARS-CoV-2 SimPLOT



- “A recent study found that a human ACE2-binding ridge in SARS-CoV-2 RBD takes a more compact conformation compared with the SARS-CoV RBD; moreover, several residue changes in SARS-CoV-2 RBD may also enhance its human ACE2-binding affinity [13]. The core residues in RBM which may relate to higher human ACE2-binding affinity than SARS-CoV are 100% identical between SARSCoV-2 and CoV-Pangolin-2020. Therefore, pangolin-CoV-2020 (CoV-pangolin/GD) potentially recognizes human ACE2 better than the SARS-CoV.”

~~SECRET//NOFORN~~

Ren et al., 2008

JOURNAL OF VIROLOGY, Feb. 2008, p. 1899–1907
0022-538X/08/\$08.00+0 doi:10.1128/JVI.01085-07
Copyright © 2008, American Society for Microbiology. All Rights Reserved.

Vol. 82, No. 4

Difference in Receptor Usage between Severe Acute Respiratory Syndrome (SARS) Coronavirus and SARS-Like Coronavirus of Bat Origin[†]

Wuze Ren,^{1†} Xiuxia Qu,^{2†} Wendong Li,^{1‡} Zhenggang Han,¹ Meng Yu,³ Peng Zhou,¹ Shu-Yi Zhang,⁴ Lin-Fa Wang,^{3*} Hongkui Deng,² and Zhengli Shi^{1*}

State Key Laboratory of Virology, Wuhan Institute of Virology, Chinese Academy of Sciences, Wuhan, China¹; Key Laboratory of Cell Proliferation and Differentiation of the Ministry of Education, College of Life Sciences, Peking University, Beijing, China²; CSIRO Livestock Industries, Australian Animal Health Laboratory and Australian Biosecurity Cooperative Research Center for Emerging Infectious Diseases, Geelong, Australia³; and School of Life Science, East China Normal University, Shanghai, China⁴

Received 20 May 2007/Accepted 15 November 2007

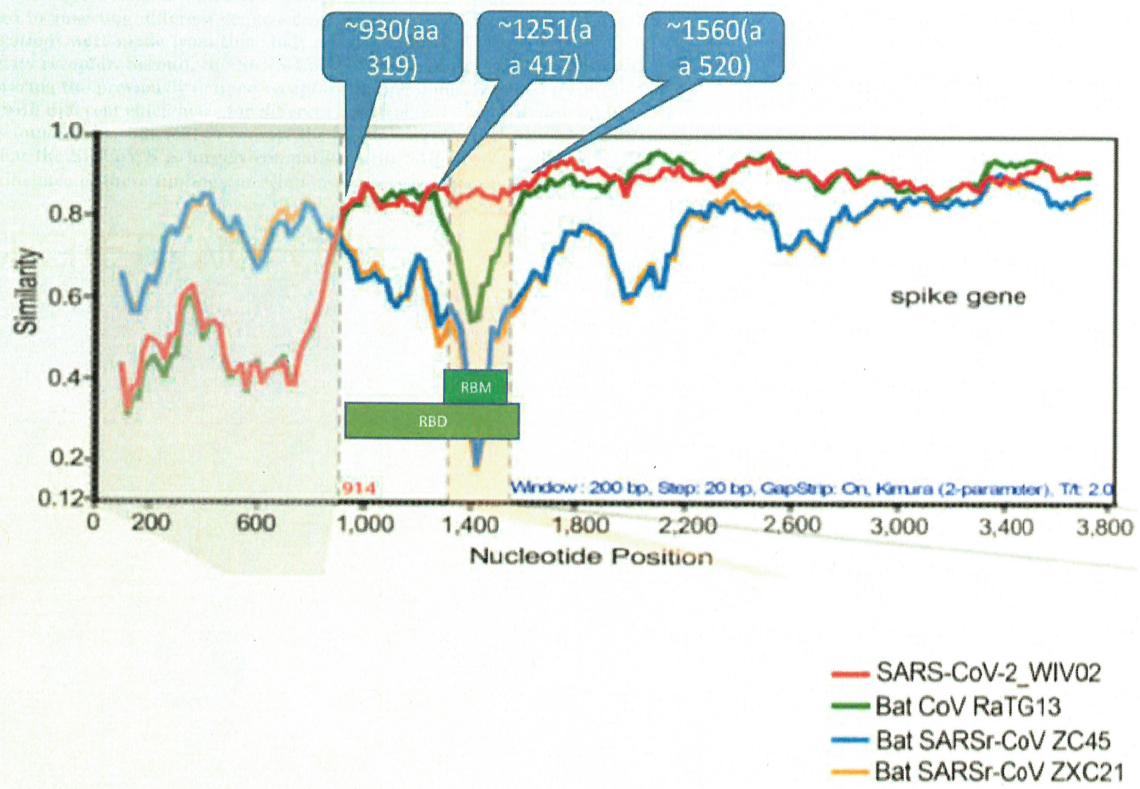
Severe acute respiratory syndrome (SARS) is caused by the SARS-associated coronavirus (SARS-CoV), which uses angiotensin-converting enzyme 2 (ACE2) as its receptor for cell entry. A group of SARS-like CoVs (SL-CoVs) has been identified in horseshoe bats. SL-CoVs and SARS-CoVs share identical genome organizations and high sequence identities, with the main exception of the N terminus of the spike protein (S), known to be responsible for receptor binding in CoVs. In this study, we investigated the receptor usage of the SL-CoV S by combining a human immunodeficiency virus-based pseudovirus system with cell lines expressing the ACE2 molecules of human, civet, or horseshoe bat. In addition to full-length S of SL-CoV and SARS-CoV, a series of S chimeras was constructed by inserting different sequences of the SARS-CoV S into the SL-CoV S backbone. Several important observations were made from this study. First, the SL-CoV S was unable to use any of the three ACE2 molecules as its receptor. Second, the SARS-CoV S failed to enter cells expressing the bat ACE2. Third, the chimeric S covering the previously defined receptor-binding domain gained its ability to enter cells via human ACE2, albeit with different efficiencies for different constructs. Fourth, a minimal insert region (amino acids 310 to 518) was found to be sufficient to convert the SL-CoV S from non-ACE2 binding to human ACE2 binding, indicating that the SL-CoV S is largely compatible with SARS-CoV S protein both in structure and in function. The significance of these findings in relation to virus origin, virus recombination, and host switching is discussed.

~~SECRET//NOFORN~~

~~SECRET//NOFORN~~

Minimal Receptor Binding Domain Cassette

- WIV scientists previously defined the minimal Receptor Binding Domain cassette that could functionally transfer ACE2 binding capability from one Spike protein to anotherSARS Nucleotide: 930-1554SARS Amino Acid: 310-518Receptor Binding MotifsSARS Nucleotide: 1251-1482SARS Amino Acid: 417-494Homology cut points of SARS-CoV-2 coincide with WIV-identified borders of RBD and RBM



Xiao *et al.*, 2020 & Ren *et al.*, 2008

~~SECRET//NOFORN~~

~~SECRET//NOFORN~~

Furin Cleavage Site

SARS-CoV CATGTCGACACTTCTATGAGTGCACATTCCATTGGAGCTGGCATTGTGCTAGTTAC
1980 H V D T S Y E C D I P I G A G I C A S Y SARS-CoV-2
CATGTCAACAACTCATATGAGTGTGACATAACCATTGGTGCAGGTATATGCGCTAGTTAT 2022
H V N N S Y E C D I P I G A G I C A S Y BCoV RaTG13
CATGTCAATAACTCGTATGAGTGTGACATAACCTATTGGTGCAGGAATATGCCAGTTAT 2022
H V N N S Y E C D I P I G A G I C A S Y SARS-CoV CATAACAGTTCTTATT-----
ACGTAGTACTAGCCAAAAATCTATTGTGGCT 2028 H T V S L L R S T S Q K S I
V ASARS-CoV-2 CAGACTCAGACTAATTCTCCTCGGCCGGCACGTAGTAGCTAGTCATCCATTGCC
2082 Q T Q T N S P R R A R S V A S Q S I I ABCoV RaTG13
CAGACTCAAACAAATTC-----ACGTAGTGTGGCCAGTCAATCTATTATTGCC 2070 Q T Q
T N S R S V A S Q S I I AFurin Cleavage SiteNmeAIII Restriction Site

A unique restriction site facilitates identifying the correct *E. coli* clone

~~SECRET//NOFORN~~

~~SECRET//NOFORN~~

SARS-CoV-2 Furin Cleavage Site GC Content

- The percent GC of the furin cleavage site insert is 77% compared to ~40% of the surrounding DNA Contains an NmeAIII restriction site The other CoV's with FCS have a %GC of <55%

Virus	Nucleotide and Amino Acid Sequences	
SARSCoV2 (47%)	GGTATATGCGCTAGTTATCAGACTCAGACTATTCTCTCGGGGGGCACTGTAGTGTAGCTAGTCATCCATTCATTGCCATACACTATG G I C A S Y Q T Q T N S P R R A R S V A S Q S I I A Y T M %GC: 14/35 = 40%	%GC: 10/13 = 77%
MERS-CoV (54%)	CTCTGTGCTCTTCCTGACACACCTAGTACTCTCACACCTCGCAGTGTGCCTCTGTTCCAGGTGAAATGCGCTTGGCATCCATTGCT L C A L P D T P S T L T P R S V R S V P G E M R L A S I A %GC: 18/35 = 51%	%GC: 8/13 = 62%
BatCoV-HKU5 (47%)	GGTCAATCACTTGTGCTATTCCACCAACTACTTCTTCACGCGTTGACGTGCTACTTCTGGTGCATCTGATGTGTTCAAATCGCC G Q S L C A I P P T T S S R V R R A T S G A S D V F Q I A %GC: 15/35 = 43%	%GC: 7/13 = 54%
IBV-Beaudette (34%)	GAAACAUASACGCAACACTAAGGMAAGGTGAGGAGTAAACGAAACGAAATTGCGATTTGTT %GC: 12/35 = 34%	%GC: 5/13 = 38%

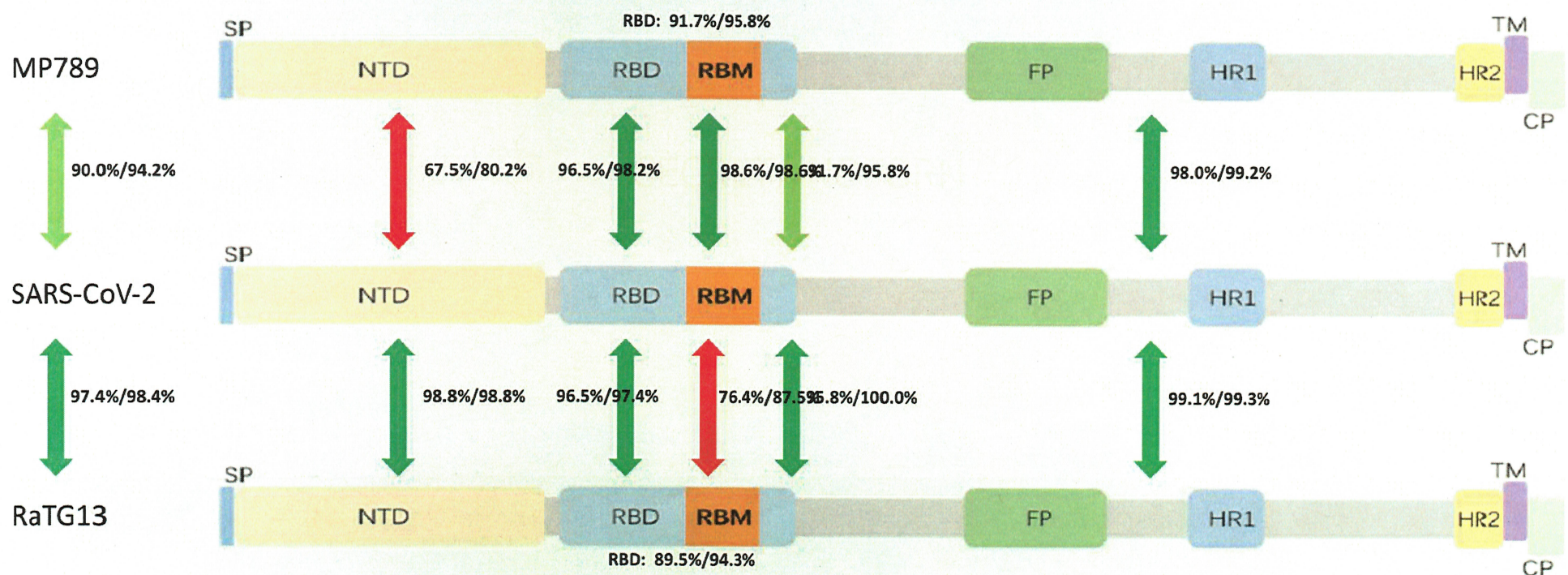
Influenza viruses convert from low path to high path by addition of a poly basic cleavage site by virtue of RNA Polymerase stuttering which adds preferentially A's and T's – this is not the case with SARS-CoV-2

~~SECRET//NOFORN~~

~~SECRET//NOFORN~~

% Identity:>95

Spike Protein Regions



~~SECRET//NOFORN~~

~~SECRET//NOFORN~~

SARS-CoV-2 Spike RBD Alignment: Possible RBM Cassette Insertion

SARSCoV2	TRFQTLLALHRSYLTGDSSSGWTAGAAAYVGYLQPRTFLLKYNENGTTDAVDCALDPBCoV_RaTG13	
TRFQTLLALHRSYLTGDSSSGWTAGAAAYVGYLQPRTFLLKYNENGTTDAVDCALDPMP789		TKFRLLTIHRGDPMP---
NNGWTVFSAAAYVGYLAPRTFMLNYNENGTTDAVDCALDP		NTD<>RBDSARSCoV2
LSETKCTLKSFTVEKG ^I YQTSNFRVQPTESIVRFPNITNLCPFGEVFNATRFASVYAWNRCoV_RaTG13		
LSETKCTLKSFTVEKG ^I YQTSNFRVQPTDSIVRFPNITNLCPFGEVFNATTFA ^S VYAWNRM ^P 789/Manis		
LSEAKCTLKS ^L TVEKG ^I YQTSNFRVQPTESIVRFPNITNLCPFGEVFNATTFA ^S VYAWN ^R SARS-CoV2		
KRISNCVADYSVLYNSASFSTFKCYGVSP ^T KLNDLCFTNVYADSFVIRGDEV ^R QIA ^P GQTBCoV_RaTG13		
KRISNCVADYSVLYNSTSFSTFKCYGVSP ^T KLNDLCFTNVYADSFVITGDEV ^R QIA ^P GQT ^M 789/Manis		
KRISNCVADYSVLYNSTSFSTFKCYGVSP ^T KLNDLCFTNVYADSFVV ^R GDEV ^R QIA ^P GQT		
>RBMSARSCoV2 GKIAD ^Y NYKLPDDFTGC ^V I ^A WNSNNLDSKVGGNNYLYRLFRKSNLKPFERDISTE ^I YQABC ^C oV_RaTG13		
GKIAD ^Y NYKLPDDFTGC ^V I ^A WNSNKHIDAKEGGNFNYLYRLFRKANLKPFERDISTE ^I YQAMP789/Manis		
GRIAD ^Y NYKLPDDFTGC ^V I ^A WNSNNLDSKVGGNNYLYRLFRKSNLKPFERDISTE ^I YQA		
RBM< RBD<SARSCoV2		
GSTPCNGVEGFNCYFPLQSYGFQPTNGVGYQPYRVVVL ^S FELLHAPATVCGPKKSTNLVKBCoV_RaTG13		
GSKPCNGQTGLNCYYPLYRYGFYPTDGVGHQPYRVVVL ^S FELLNAPATVCGPKKSTNLVKMP789/Manis		
GSTPCNGVEGFNCYFPLQSYGFHPTNGVGYQPYRVVVL ^S FELLNAPATVCGPKQSTNLVK SARS-CoV2		
NKCVNFNFNGLTGTGV ^L TESNKKFLPFQQFGRDIADTTDAVRDPQTLEILDITPCSFGGVBCoV_RaTG13		
NKCVNFNFNGLTGTGV ^L TESNKKFLPFQQFGRDIADTTDAVRDPQTLEILDITPCSFGGVMP789		
NKCVNFNFNGLTGTGV ^L TESSKKFLPFQQFGRDIADTTDAVRDPQTLEILDITPCSFGGV		

ACE2 Critical Contact ACE2

~~SECRET//NOFORN~~

~~SECRET//NOFORN~~

SARS-CoV-2 RBD vs PCoV MP789 RBD

>RBM

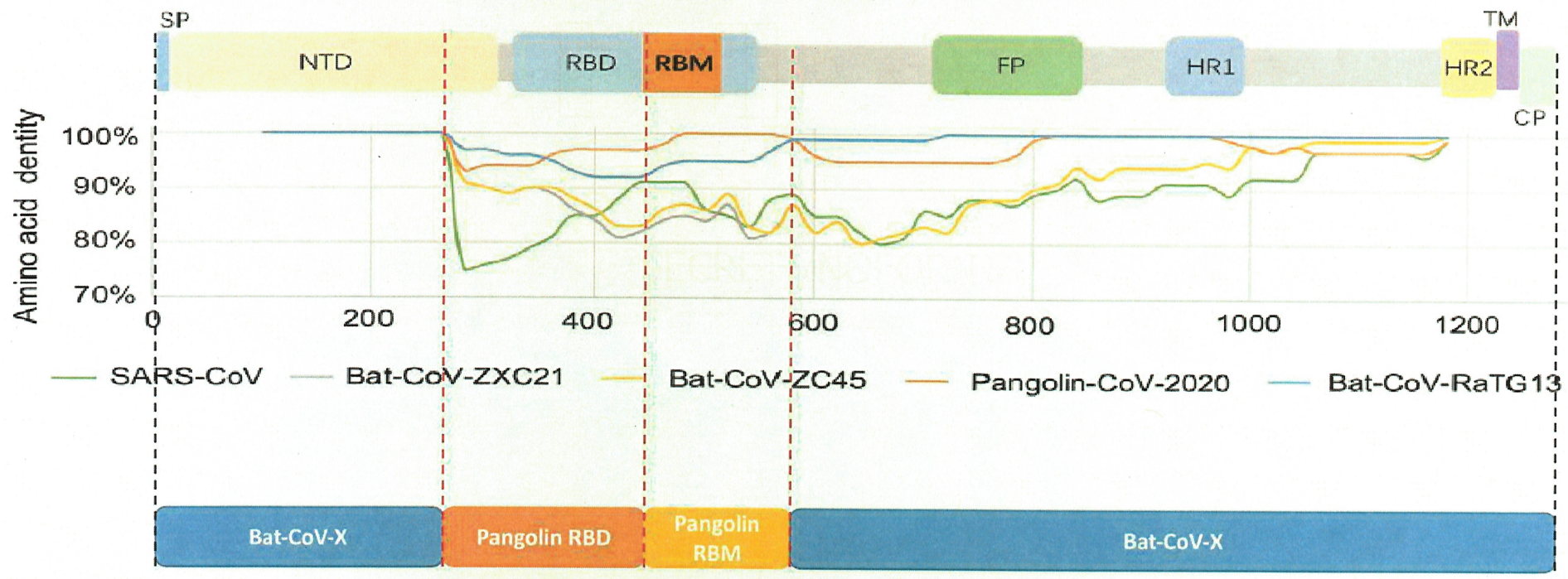
D Y N Y K L P D D F T G C V I A W N S N MP789
GACTATAATTAAACCTCCGTGATGATTTCACAGGTTGTAATAGCTTGGAAATTCTAAC 1305SARSCOV2
GATTATAATTAAATTACAGATGATTTCACAGGCTGCCTTATAGCTTGGAAATTCTAAC 1317 D
Y N Y K L P D D F T G C V I A W N S N N L D
S K V G G N Y N Y L Y R L F R K S MP789
AACCTTGATTCTAAGGTTGGTGGTAATTATAACTACCTTATAGATTGTTAGAAAGTCC 1365SARSCOV2
AATCTTGATTCTAAGGTTGGTGGTAATTATAATTACCTGTATAGATTGTTAGGAAGTCT 1377 N
L D S K V G G N Y N Y L Y R L F R K S N L K
P F E R D I S T E I Y Q A G S T P MP789
AACCTCAAAACCTTTGAACGAGACATTCTACAGAAATATACCAAGCTGGTAGTACACCC 1425SARSCOV2
AATCTCAAAACCTTTGAGAGAGATATTCAACTGAAATCTATCAGGCCGGTAGCACACCT 1437 N
L K P F E R D I S T E I Y Q A G S T P C N G
V E G F N C Y F P L Q S Y G F Q P MP789
TGCAATGGGTTGAAGGTTTAACTGTTACTTCCTCTACAATCTTATGGTTCCACCT 1485SARSCOV2
TGTAAATGGTGTGAGGTTTAATTGTTACTTCCTTACAATCATATGGTTCCAACCC 1497 C
N G V E G F N C Y F P L Q S Y G F Q P
RBM< T N G V G Y Q P Y R V V V L S F E L L H
MP789 ACTAATGGTGTGGTACCAACCTTATAGAGTAGTAGTATTGTCAATTGAACCTTTAAAAA
1545SARSCOV2
ACTAATGGTGTGGTACCAACCATAACAGAGTAGTAGTACTTCTTTGAACCTCTACAT 1557 T
N G V G Y Q P Y R V V V L S F E L L K
RBD< A P A T V C G P K K S T N MP789
GCACCTGCTACTGTTGTGGACCTAACAGTCCACTAACCTAGTTAAAAACAAAATGTGTC 1605SARSCOV2
GCACCAGCAACTGTTGTGGACCTAAAAGTCTACTAATTGGTTAAAACAAATGTGTC 1617 A
P A T V C G P K K S T N

- 38 codon differencesFirst:
4Second: 0Third: 31First
and third: 31 results in an
amino acid changePangolin
RBD cassette appears to be
a codon optimized insert

~~SECRET//NOFORN~~

~~SECRET//NOFORN~~

SARS-CoV-2 Spike Appears to be a Chimera

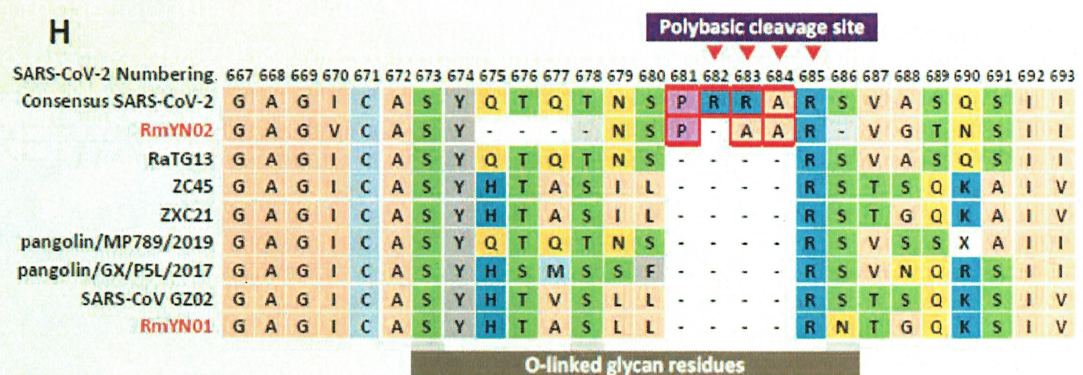


Break points align with those identified by WIV Scientists in
2008 (Ren *et al.*, 2008)

~~SECRET//NOFORN~~

RmYN02 - A Red Herring?

- Zhou et al., 2020 publish paper describing Bat CoV rmYN02Next generation sequencing was done on pooled bat samples to develop two genome sequences – RmYN01 and RmYN02Claim that RmYN02 contains inserted nucleotides at the S1/S2 cleavage siteAssert that the SARS-CoV-2 FCS is therefore of natural originNo virus is available for peer confirmation



~~SECRET//NOFORN~~

Zhou et al., 2020

~~SECRET//NOFORN~~

RmYN02 - A Red Herring?

Virus	Nucleotide Sequences
SARSCoV2	GGTATATGCGCTAGTTATCAGACTCAGACTAAATTCTCCCTCGGGGGCACGTAGTGTAGCTAGTCATACTCCATCATTGCCTACACTATG
RaTG13	GGAATATGCGGCCAGTTATCAGACTCAAACCTAATTCA~~~~~CGTAGTGTGGCCAGTCAATCTATTATTGCCTACACTATG
P-CoV MP789	GGAATATGTGCCAGTTATCAGACTCAAACCTAATTCA~~~~~CGTAGTGTGGCAAGTCAAGCTATTATTGCCTACACTATG
RmYN02	GGTGTGTGCCAGTTACAACCTCACCTGCAGCG~~~~~CGTAGTGTGGCAAGTCAAGCTATTATTGCCTACGGATG
ZC45	GGTATTTGTGCTAGCTACCATACGGCTTCTATATTAA~~~~~CGCAGTACAAGGCCAGAAAGCTATTGTGGCTTATACTATG
ZXC21	GGTATTTGTGCTAGCTACCATACGGCTTCTATATTAA~~~~~CGTAGTACAGGGCCAGAAAGCTATTGTGGCTTATACTATG
SARSCoV	GGCATTTGTGCTAGTTACCATACAGTTCTTATTAA~~~~~CGTAGTACTAGCCAAAAATCTATTGTGGCTTATACTATG

~~SECRET//NOFORN~~

~~SECRET//NOFORN~~

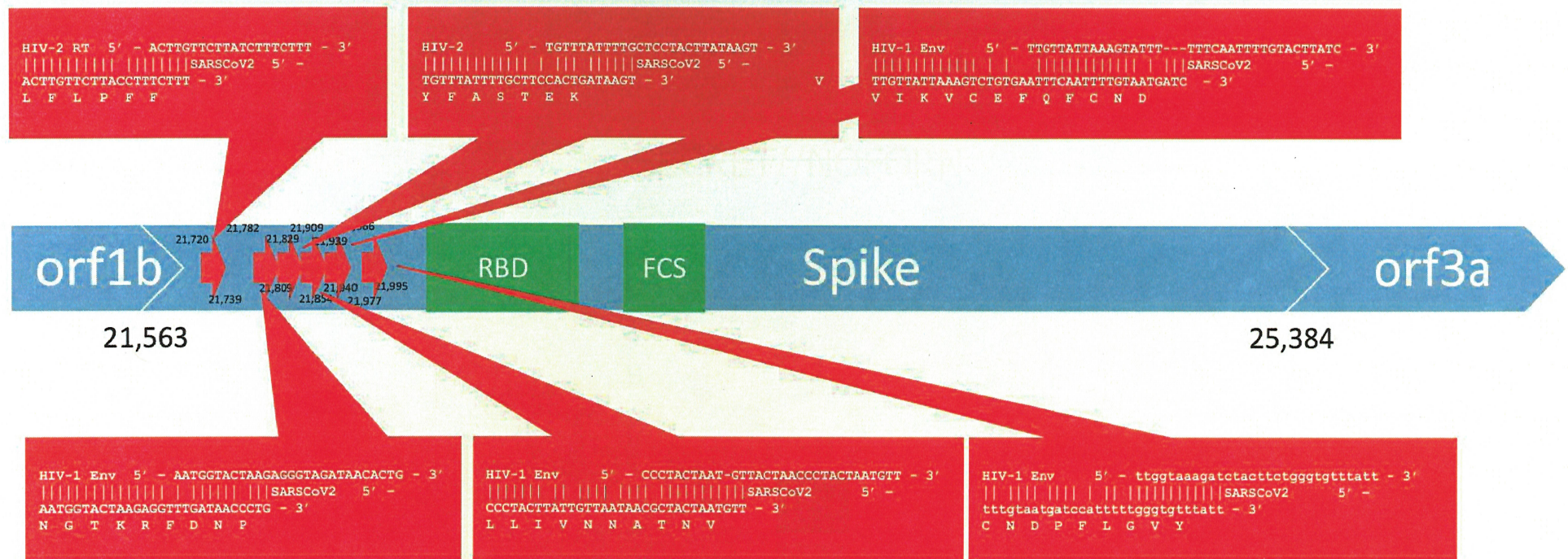
HIV Epitopes

Perez, 2020

~~SECRET//NOFORN~~

~~SECRET//NOFORN~~

HIV Sequences in the SARS-CoV-2 Spike Gene



Adapted from Perez, 2020

~~SECRET//NOFORN~~

~~SECRET//NOFORN~~

Perez, 2020 Scientific Challenges

- None of the six proposed regions are identical at either the nucleotide or amino acid level with the corresponding HIV/SIV segmentsNone of the six peptides are related to identified immunosuppressive regions of HIV and SIV (Retroviral ISU Domains)The HIV gp41 Immunosuppressive (ISU) Domains sequence is KQLQARILAVERYLKDQQLLGG - this sequence does not match any of the sixFour of the six regions either perfectly or almost perfectly match corresponding peptides in multiple Pangolin CoVs - Perez did not account for Pangolin genomes in the paperSeveral are only found in Pangolin CoV Spike sequences and not in Bat CoV Spike sequences, indicating that the SARS-CoV-2 Spike NTD region originated from a Pangolin CoV template

The next 2 pages are DIF citing (b)(1) and (b)(3) and are not provided.

~~SECRET//NOFORN~~

~~SECRET//NOFORN~~

Alternative Scenario

~~SECRET//NOFORN~~

~~SECRET//NOFORN~~

Hypothetical Laboratory Origin of SARS-CoV-2

- WIV conducted a longitudinal studies to isolate a large number of bat Coronaviruses from multiple locations in China (2011-2015)WIV Developed Reverse Genetic System, assembled WIV1 full-length infectious clone, and created chimeric viruses exchanging the WIV1 spike gene with the spike gene from other bat Coronaviruses (2015-2017)WIV and other Chinese scientists conduct gain of function studies on SARS, MERS, IBV, and PEDV to insert furin cleavage sites demonstrating increased virulence of the chimeric virusesWIV conducted in vivo and in vitro studies to characterize the bank of bat CoronavirusesWIV conducted the live bat Coronavirus studies under BSL2 conditionsChinese BSL2 and US BSL2 conditions are differentChinese labs have had a history of virus escapes from BSL2 laboratoriesHypothesis: Between 2017 and 2019, WIV created a full-length infectious clone in pBAC-CMV using an unpublished bat Coronavirus genome as template (BatCoVX)Hypothesis: Between 2017 and 2019, WIV created chimeric Bat-CoV-X viruses using the pBAC-CMV-BCoVX backbone and swapping out key cassettes with other bat Coronaviruses (RBD, RBM, etc.) and adding additional features such as a furin cleavage siteHypothesis: In 2018-2019, WIV conducted in vitro and in vivo studies to characterize the BatCoVX chimeric viruses under BSL2 conditionsHypothesis: In mid-2019, one of the not fully characterized Bat-CoV-X chimeric viruses escaped from the WIV facilities and begins infecting civilians in the city of WuhanHypothesis: Starting in mid-2019 through present, WIV and other Chinese laboratories conduct studies to characterize the Chimerc BCoVX virus that escaped (now called SARS-CoV-2)WIV (Zhou et al., 2020) publishes the 2019-nCoV genome sequence showing relatedness to RaTG13 (a previously unpublished genome)BatCoVX likely highly related to RaTG13Hypothesis: Beginning in early 2020, WIV and other government controlled agencies begin to publish obfuscation information to drive the narrative that SARS-CoV-2 is of natural origin and resulted from natural recombinationRaTG13RMYN02Pangolin CoV's

~~SECRET//NOFORN~~

~~SECRET//NOFORN~~

CONCLUSION

The next page is DIF citing (b)(1) and (b)(3) and is not provided.

~~SECRET//NOFORN~~

~~SECRET//NOFORN~~

Concluding Points

- WIV possesses a bank of Bat Coronavirus isolatesWIV has scientists experienced in Coronavirology and Coronavirus Infectious Clone generationWIV Scientists generated chimeric SARS CoV and Bat CoV Spike genes to identify minimal Spike Receptor Binding Domain cassette that could transfer receptor binding specificity (Ren et al., 2008)WIV possesses an existing and published Coronavirus Reverse Genetics System (Zeng et al., 2016) utilizing their pBAC-CMV plasmidWIV has utilized the pBAC-CMV-WIV1 Full-length clone to generate chimeras with Bat CoV spike genes (Hu et al., 2017)WIV has BSL2/BSL3/BSL4 animal facilitiesWIV has multiple in vitro assays (apoptosis, IFN-B induction, etc.) to characterize their Bat Coronaviruses and chimeric Bat CoronavirusesWIV and other Chinese researchers have conducted Gain of Function studies in SARS, MERS, IBV, and PEDV to add Furin Cleavage Sites to CoV Spike proteinThe absence of a published progenitor virus for SARS-CoV-2 only indicates that it has not been published, not that it does not existThe genomic sequence of SARS-CoV-2 has Type IIS restriction sites that are consistent with being generated by the Golden Gate Cloning system utilizing the published pBAC-CMV plasmidThe SARS-CoV-2 genome has several break points where homology jumps from Bat Coronaviruses to Pangolin Coronaviruses which is consistent with a synthesized chimeric virusThe SARS-CoV-2 Spike protein similarity with RaTG13 and Pangolin CoV Spike proteins may also be explained by use of cassettes swapped into the base virus – these break points align with those identified by WIV scientists (Ren et al., 2008)The Pangolin RBD cassette is 100% identical at the amino acid level while the DNA sequence appears to be codon optimizedThere are no other published SARS lineage Betacoronaviruses that possess a Furin Cleavage Site in their Spike protein (RmYN02 does not have an insertion) and the SARS-CoV-2 FCS does not appear to be inserted via the same mechanism that drives Influenza virus insertions of polybasic cleavage sitesZeng et al., 2016 stated that "All experiments using live virus was conducted under biosafety level 2 (BSL2) conditions" which would make an accidental release of a pathogenic Bat CoV capable of binding human ACE2 more likelyA chimeric virus comprised of segments from natural Bat CoV genomes would appear like a recombined virus

The molecular biology capabilities of WIV and the genome assessment are consistent with the hypothesis that SARS-CoV-2 was a lab-engineered virus that was part of a bank of chimeric viruses in Zhen-Li Shi's laboratory at WIV that escaped from containment

~~SECRET//NOFORN~~

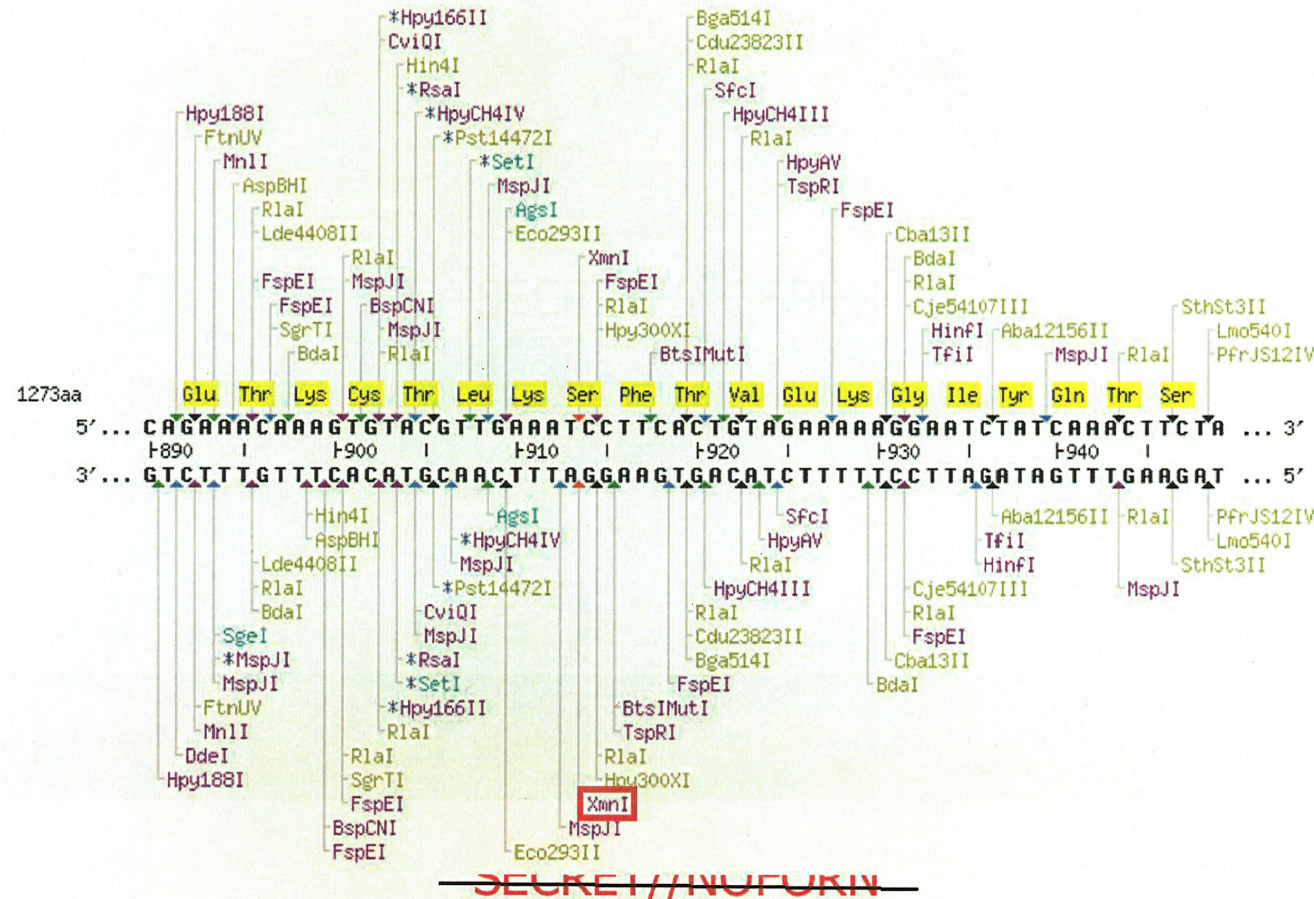
~~SECRET//NOFORN~~

BACK-UP SLIDES

~~SECRET//NOFORN~~

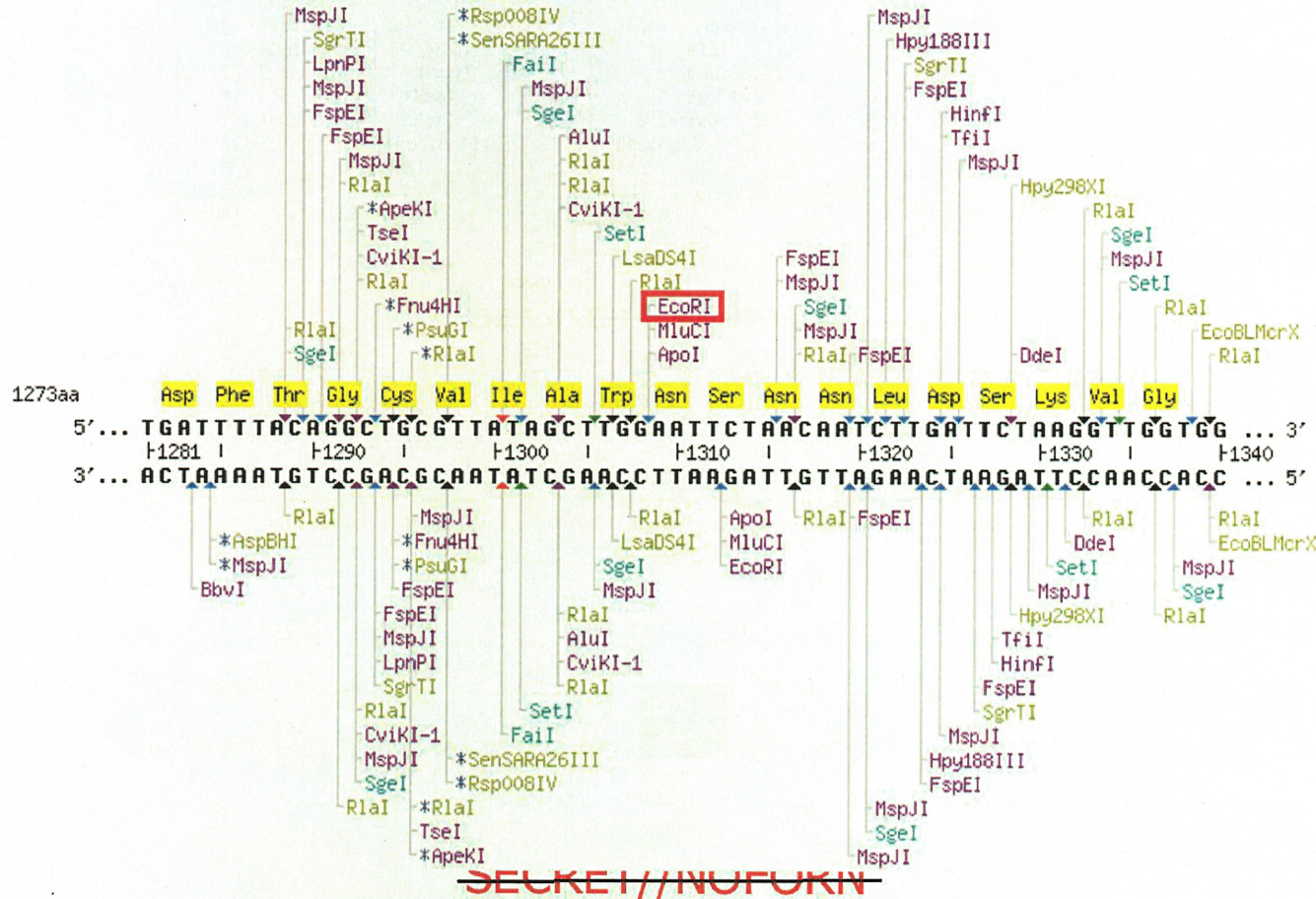
~~SECRET//NOFORN~~

Nucleotide 914 Region



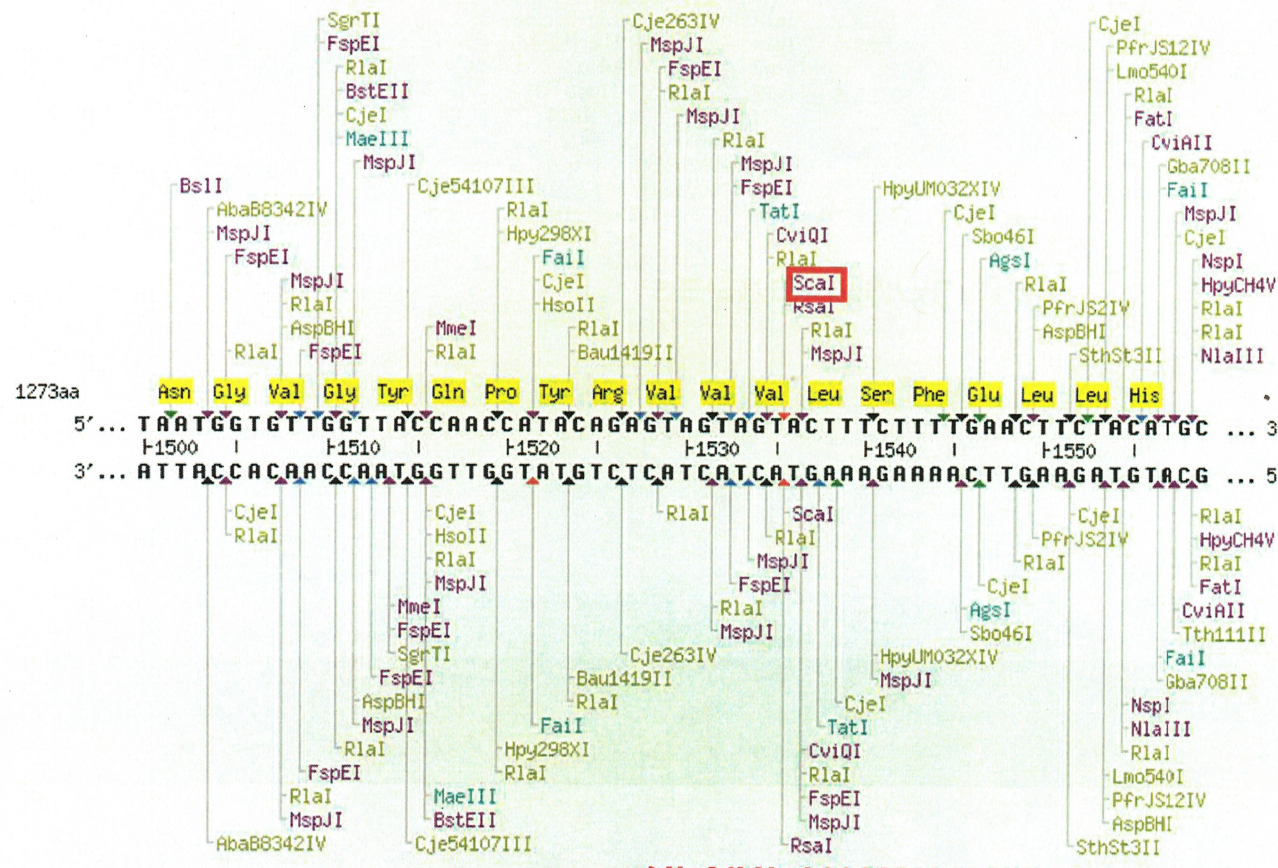
~~SECRET//NOFORN~~

Nucleotide 1312 Region



~~SECRET//NOFORN~~

Nucleotide 1535 Region



~~SECRET//NOFORN~~

SARS-CoV CATGTCGACACTTCTTATGAGTGCACATTCCCTATTGGAGCTGGCATTGTGCTAGTTAC
1980 H V D T S Y E C D I P I G A G I C A S Y SARS-CoV-2
CATGTCAACAACTCATATGAGTGTGACATACCCATTGGTGCAGGTATATGCGCTAGTTAT 2022
H V N N S Y E C D I P I G A G I C A S Y BCoV RaTG13
CATGTCAATAACTCGTATGAGTGTGACATACCTATTGGTGCAGGAATATGCCAGTTAT 2022
H V N N S Y E C D I P I G A G I C A S Y SARS-CoV CATACAGTTCTTATT-----
ACGTAGTACTAGCCAAAAATCTATTGTGGCT 2028 H T V S L L R S T S Q K S I
V ASARS-CoV-2 CAGACTCAGACTAATTCTCCTCGGCAGGTAGTGTAGCTAGTCATCCATCATTGCC
2082 Q T Q T N S P R R A R S V A S Q S I I ABCoV RaTG13
CAGACTCAAACAAATTC-----ACGTAGTGTGGCCAGTCAATCTATTATTGCC 2070 Q T Q
T N S R S V A S Q S I I AFurin Cleavage SiteBspMI Restriction SiteNmeAIII Restriction SiteBsrDI
Restriction Site

~~SECRET//NOFORN~~